(Fig. 1a).[7,8] A key component of the traceable linker is a stimulus-responsive amino acid that possesses a stimulus-removable protective group (PG) on the phenolic hydroxyl group (Fig. 1b).[9] The stimulus-responsive amino acid induces amide bond cleavage after stimulus-induced removal of the PG and subsequent lactonization of a trimethyl lock moiety.[10] In a previous report, the traceable linker composed of a thiol-responsive amino acid, in which the PG is a *p*-nitrobenzenesulfonyl (*p*Ns) group, was presented (Fig. 1a). The traceable linker was introduced onto an alkynylated protein by click chemistry and then adsorbed onto the streptavidin beads. Subsequent addition of a thiol triggered the cleavage of the linker to release the protein possessing an aminooxy group. Since the aminooxy group can react with an aldehyde chemoselectively,[11] the eluted target protein was selectively labeled with an aldehyde-containing labeling reagent even when contaminated non-target proteins co-existed. As the thiol was used as the cleavage inducer in this system, it is preferable to remove endogenous thiols, such as glutathione before the use of the thiol-responsive traceable linker.[12] To avoid the risk of unintentional cleavage of the traceable linker, in this study, we have developed a fluoride-responsive (FR) traceable linker, because there are few fluoride ions present in a living body.[13]

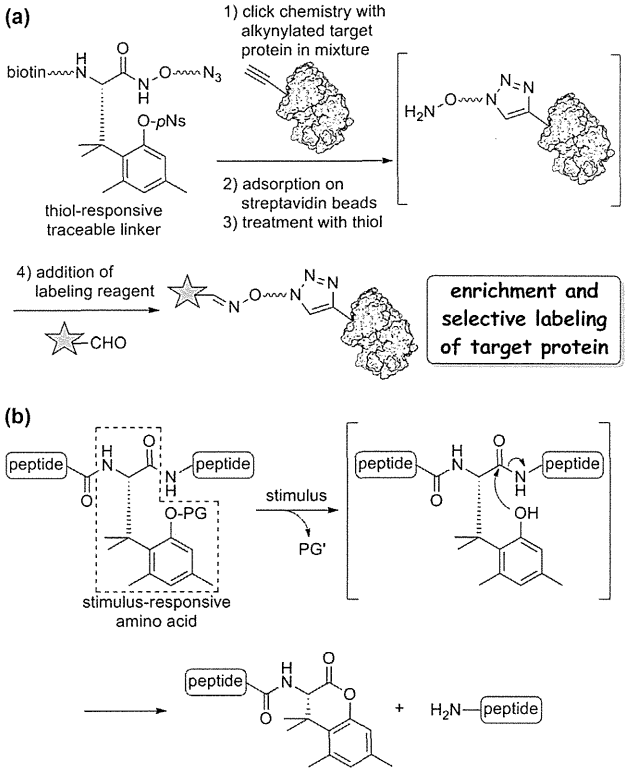

Fig. 1. Molecular design. (a) Purification and selective labeling of an alkynylated protein using a thiol-responsive traceable linker (*p*Ns: *p*-nitrobenzenesulfonyl group). (b) A stimulus-responsive amide bond cleavage system (PG: protective group i.e., removable by appropriate stimulus).

2. Results and discussion

2.1. Synthesis of an FR amino acid

Preparation of the FR amino acid possessing a fluoride-removable protective group as the PG of the stimulus-responsive amino acid was attempted. A *tert*-butyldiphenylsilyl (TBDPS) group was chosen as the fluoride-removable PG because acid treatment is unavoidable for the synthesis of the traceable linker and the TBDPS group is relatively acid tolerant compared with other trisubstituted silyl protections.[14] In this study, Fmoc protected derivatives were designed for Fmoc-based solid phase peptide synthesis (Fmoc SPPS). We first attempted to synthesize silyl ether **1**, but introduction of the TBDPS group onto the phenolic hydroxyl group of **2**[15] did not proceed (Fig. 2). In these reactions, recovery of the starting material, removal of the Boc group and/or removal of the *tert*-butyldimethylsilyl (TBS) group were observed. We speculated that the direct introduction of the TBDPS group onto the phenol is sterically unfavorable and steric crowding around the phenol was observed in an energy minimized structure of substrate **2** using an MM2 calculation (Fig. S1). Therefore, preparation of **3** possessing a sterically less demanding siloxybenzyl unit, which can be removed via fluoride-induced cleavage of the silyl group followed by release of the quinone methide, onto the phenol was next examined (Scheme 1).[16] Starting from phenol **2**, it was subjected to the modified Mitsunobu reaction with the TBDPS derivative **4**[17] using *N,N,N′,N′*-tetramethylazodicarboxamide (TMAD).[18] The TBS group of **5** was then removed under acidic conditions to yield alcohol **6**. After stepwise oxidation of the alcohol of **6**, the Boc group was removed by the use of Ohfune's protocol,[19] because cleavage of the *p*-siloxybenzyl group was observed when trifluoroacetic acid (TFA) or hydrogen chloride was employed. The obtained amine was finally protected with an Fmoc group to yield FR amino acid **3**.

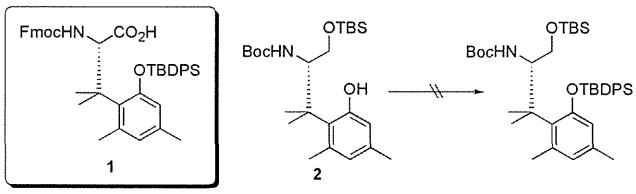

Entry	Attempted reaction conditions
1	TBDPSCl, imidazole, DMF
2	TBDPSCl, imidazole, DMF, 60 °C
3	TBDPSOTf, 2,6-lutidine, CH_2Cl_2
4	TBDPSCl, LiHMDS, THF
5	TBDPSCl, NaH, DMF
6	TBDPSCl, $AgNO_3$, DMF
7	TBDPSCl, $AgNO_3$, pyridine, 60 °C

Fig. 2. Synthetic attempts to prepare FR amino acid **1** (LiHMDS: lithium hexamethyldisilazide; TBDPSOTf *tert*-butyldiphenylsilyl trifluoromethanesulfonate).

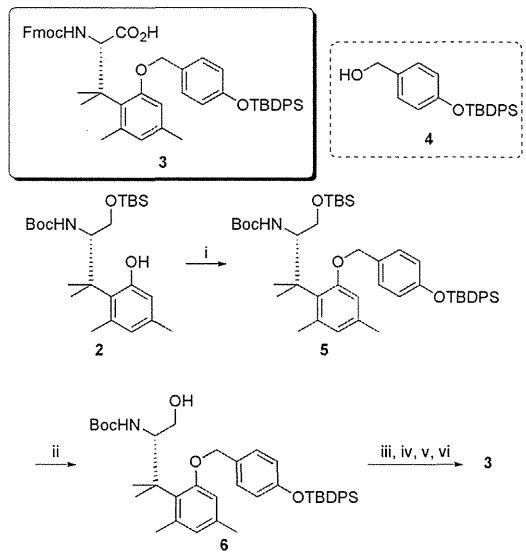

Scheme 1. Reagents and conditions: (i) **4**, TMAD, *n*-Bu_3P, toluene, 98%; (ii) AcOH, THF, H_2O, quant.; (iii) oxalyl chloride, DMSO, Et_3N, THF; (iv) $NaClO_2$, NaH_2PO_4, 2-methyl-2-butene, *tert*-BuOH, acetone, H_2O; (v) *tert*-butyldimethylsilyl trifluoromethanesulfonate (TBSOTf), 2,6-lutidine, CH_2Cl_2; (vi) FmocOSu, Na_2CO_3, acetonitrile (MeCN), H_2O, 43% (four steps).

2.2. Preparation of an FR traceable linker

FR traceable linker **7** was prepared using Fmoc SPPS (Scheme 2). Release of the linker from the resin using standard TFA conditions was not compatible because of acid lability of the siloxybenzyl unit. A 2-chlorotrityl resin from which the product can be released by treatment with a weak acid was therefore suitable for this synthesis and a commercially available amino acid-preloaded resin was employed to avoid laborious attachment of the first amino acid on the resin. Starting from the glycine-preloaded 2-chlorotrityl resin, azide derivative **8**[20] and aminooxy derivative **9**[21] were incorporated by standard Fmoc SPPS conditions using *N,N′*-diisopropylcarbodiimide (DIC)/1-hydroxybenzotriazole (HOBt) system. After coupling of FR amino acid **3** in the presence of *O*-(7-azabenzotriazol-1-yl)-*N,N,N′,N′*-tetramethyluronium hexafluorophosphate (HATU) and *N,N*-diisopropylethylamine (DIEA), miniPEG unit **10** and biotin were incorporated using the DIC/HOBt system. The resin was finally treated with a 2,2,2-trifluoroethanol (TFE)/AcOH/CH_2Cl_2 cocktail to generate FR traceable linker **7** without accompanying the deprotection of the siloxybenzyl unit (12% all over yield. An HPLC chart of the product is shown in Fig. S2 in the Supplementary data).

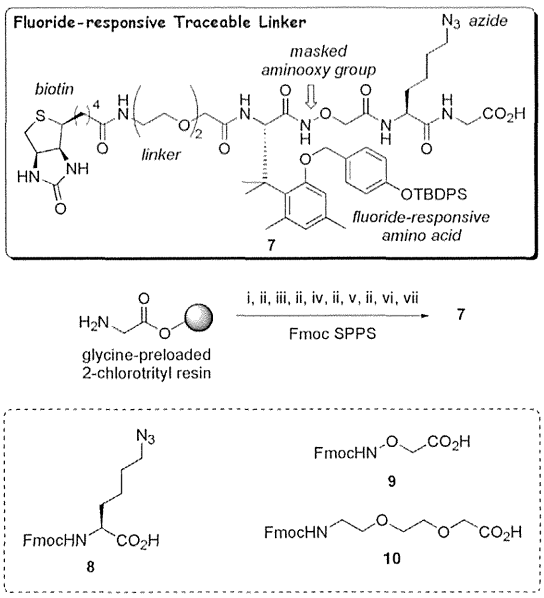

Scheme 2. Reagents and conditions: (i) **8**, HOBt·H_2O, DIC, DMF; (ii) 20% (v/v) piperidine in DMF; (iii) **9**, HOBt·H_2O, DIC, DMF; (iv) **3**, HATU, DIEA, DMF; (v) **10**, HOBt·H_2O, DIC, DMF; (vi) biotin, HOBt·H_2O, DIC, DMF; (vii) TFE/AcOH/CH_2Cl_2=1/1/3 (v/v).

2.3. Click chemistry, fluoride-induced cleavage, and selective labeling of the FR traceable linker with a model peptide

In this study, alkyne-containing peptide **11**[7] was employed as a model of the alkynylated target protein because of ease of handling and characterization of products (Fig. 3). *tert*-Butanol was used as a cosolvent to dissolve the traceable linker. Traceable linker **7** and model peptide **11** in an aqueous *tert*-butanol solution were treated with $CuSO_4$ and sodium ascorbate. Following a reaction time of 1 h, completion of the coupling and production of conjugate **12** in high purity were confirmed by HPLC monitoring.

Fluoride-induced cleavage of the linker moiety of peptide conjugate **12** followed by the labeling reaction was next examined (Fig. 4). Conjugate **12** was dissolved in a phosphate buffer containing 0.1 M KF, 100 equiv of 2-mercaptoethanesulfonic acid sodium salt (MESNa) as a scavenger of quinone methide generated via removal of the siloxybenzyl unit, 6 M guanidine hydrochloride, and

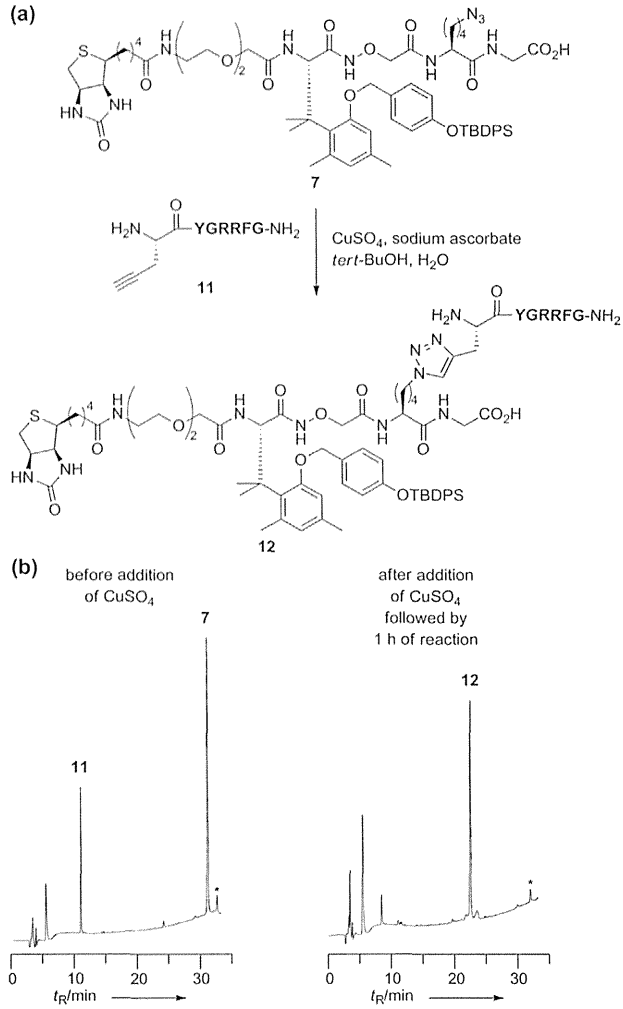

Fig. 3. Click chemistry of the traceable linker. (a) Reaction of traceable linker **7** with model peptide **11**. (b) HPLC monitoring of the click chemistry. HPLC conditions: Cosmosil $5C_{18}$-AR-II analytical column, linear gradient of 0.1% (v/v) TFA/MeCN in 0.1% (v/v) TFA aq, 5–90% over 30 min. *Non-peptidic compound.

0.05 mM EDTA (0.2 M phosphate, pH 7.6), and the reaction mixture was incubated at 37 °C. The silyl group was completely removed after 2 h of the reaction. Following the additional 10 h of incubation, intermediate **13** was cleaved to generate biotin derivative **14** and aminooxy derivative **15**. These results suggest that a rate determining step of the reaction is the removal of the quinone methide. The reaction mixture was then subjected to subsequent labeling without purification. We used 3-bromobenzaldehyde as the labeling reagent, because the labeled compounds can easily be distinguished based on an isotope pattern of the MS.[6b,22] To the reaction mixture was added 3-bromobenzaldehyde and the labeling was accomplished within 5 min. Although **15** possesses a free amino group at the N-terminus of the peptide, incorporation of two aldehydes was not observed. This result demonstrates that the selective labeling of the aminooxy group with the aldehyde was achieved.[23]

3. Conclusion

Preparation of the FR amino acid and its application to the FR traceable linker were reported. The traceable linker was successfully introduced onto an alkyne-containing model peptide using click chemistry, and fluoride-induced cleavage followed by selective labeling of the obtained traceable linker-model peptide conjugate was achieved. Its application to the isolation and selective

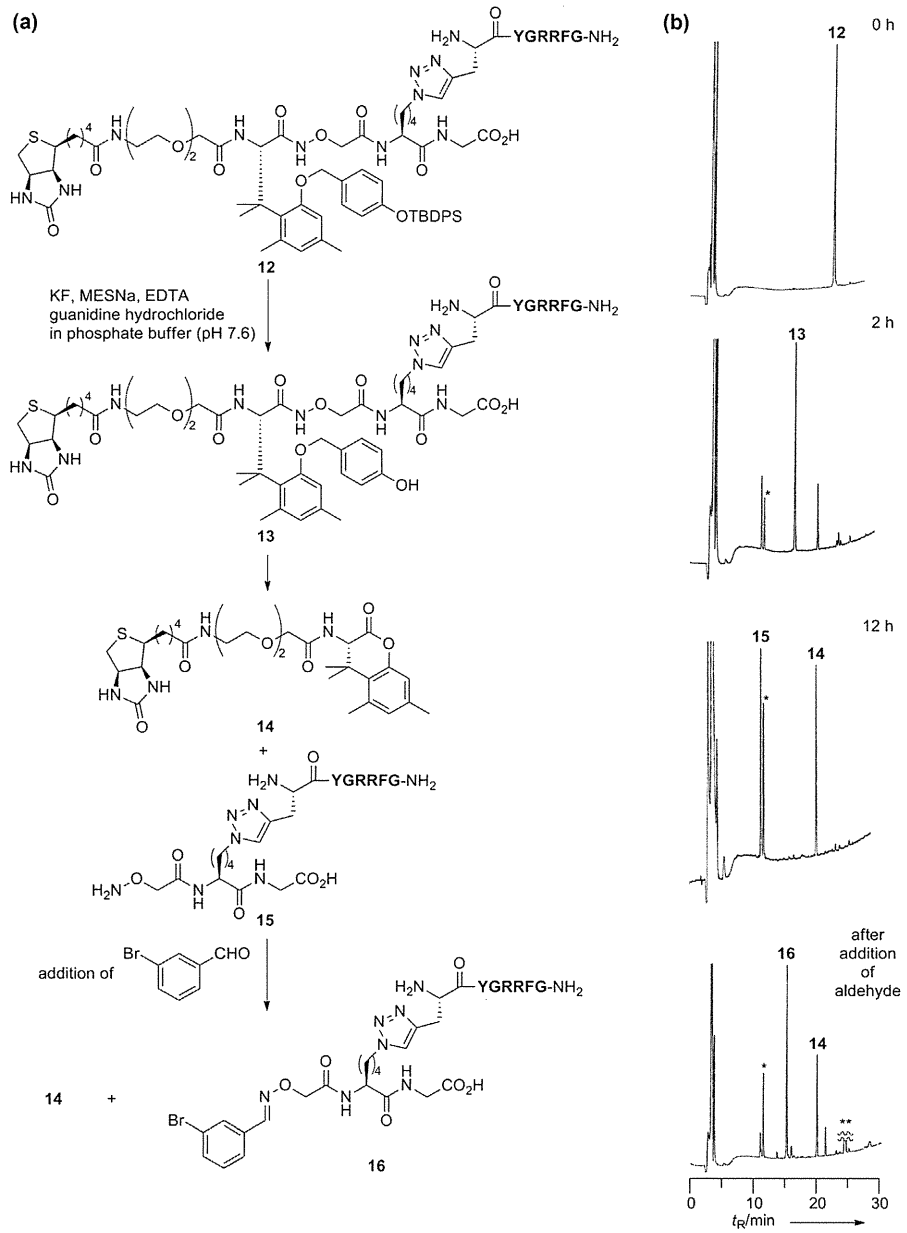

Fig. 4. Fluoride-induced cleavage of the traceable linker followed by selective labeling. (a) Treatment of the traceable linker-peptide conjugate **12** with KF followed by labeling with 3-bromobenzaldehyde. (b) HPLC monitoring of the reactions. HPLC conditions: Cosmosil $5C_{18}$-AR-II analytical column, linear gradient of 0.1% (v/v) TFA/MeCN in 0.1% (v/v) TFA aq, 5–90% over 30 min. *Non-peptidic compound derived from the quinone methide.[24] **3-Bromobenzaldehyde.

labeling of alkynylated target proteins is currently underway in our laboratory.

4. Experimental section

4.1. General methods

All reactions of small molecules were carried out under a positive pressure of argon at room temperature unless otherwise noted. For column chromatography, silica gel (KANTO KAGAKU N-60) was employed. Mass spectra were recorded on a Waters MICROMASS® LCT PREMIER™ or a Bruker Esquire200T. NMR spectra were measured using a JEOL GSX400 or a JEOL GSX300 spectrometer. For HPLC separations, a Cosmosil $5C_{18}$-AR-II analytical column (Nacalai Tesque, 4.6×250 mm, flow rate 1.0 mL/min) or a semi-preparative column (10×250 mm, flow rate 3 mL/min) was employed, and eluting products were detected by UV at 220 nm. A solvent system consisting of 0.1% (v/v) TFA in H_2O (solvent A) and 0.1% TFA (v/v) in MeCN (solvent B) was used for HPLC elution. IR spectra and optical rotations were measured using a JASCO FT-IR 6200 and a JASCO P-2200 polarimeter (concentration in g/100 mL), respectively. A melting point was determined on a YAMATO-MODEL 20 melting point apparatus and was uncorrected. An elemental analysis was performed using a J-SCIENCE LAB JM10.

4.2. Synthesis of FR amino acid derivatives

*4.2.1. (S)-tert-Butyl [1-{(tert-butyldimethylsilyl)oxy}-3-{2-([4-{(tert-butyldiphenylsilyl)oxy}benzyl]oxy)-4,6-dimethylphenyl}-3-methylbutan-2-yl]carbamate (**5**).* To a stirred solution of phenol **2**[15] (200 mg, 0.457 mmol), benzyl alcohol **4**[17] (250 mg,

0.690 mmol), and TMAD (236 mg, 1.37 mmol) in toluene (4.6 mL) was added tri-*n*-butylphosphine (342 μL, 1.37 mmol) at 0 °C. After being stirred at same temperature for 30 min, the resulting mixture was additionally stirred at room temperature for 3 h. Following to the addition of water, the mixture was extracted with EtOAc. The organic layer was washed with brine, dried over Na_2SO_4, and concentrated in vacuo. The crude product was purified by column chromatography (hexanes/EtOAc=20/1 (v/v)) and 349 mg of ether **5** (0.446 mmol, 98%) was obtained as a colorless oil: $[\alpha]_D^{20}$ −22.3 (*c* 1.29, $CHCl_3$); ^1H NMR ($CDCl_3$, 400 MHz) δ=−0.06 (3H, s), −0.04 (3H, s), 0.86 (9H, s), 1.13 (9H, s), 1.40 (9H, s), 1.49 (3H, s), 1.50 (3H, s), 2.20 (3H, s), 2.55 (3H, s), 3.47 (1H, dd, *J*=10.6 and 5.0 Hz), 3.56 (1H, dd, *J*=10.6 and 4.0 Hz), 4.54 (1H, ddd, *J*=10.0, 5.0, and 4.0 Hz), 4.85 (1H, d, *J*=10.0 Hz), 4.94 (1H, d, *J*=11.6 Hz), 4.99 (1H, d, *J*=11.6 Hz), 6.55 (1H, s), 6.57 (1H, s), 6.78 (2H, d, *J*=8.5 Hz), 7.21 (2H, d, *J*=8.5 Hz), 7.35–7.47 (6H, m), 7.71–7.77 (4H, m); ^{13}C NMR ($CDCl_3$, 75 MHz) δ=−5.6, −5.5, 18.1, 19.5, 20.7, 25.8, 25.8, 26.5, 27.7, 28.4, 29.3, 44.5, 56.7, 63.6, 70.7, 78.3, 112.7, 119.7, 127.4, 127.7, 128.6, 129.8, 130.0, 131.0, 132.9, 135.5, 136.0, 138.5, 155.1, 156.0, 158.7; IR (neat) 701, 835, 919, 1113, 1172, 1255, 1511, 1610, 1700, 1721, 2858, 2930, 2957 cm^{-1}; HRMS (ESI-TOF) *m/z* calcd for $C_{47}H_{68}NO_5Si_2$ ($[M+H]^+$) 782.4636, found 782.4610.

*4.2.2. (S)-tert-Butyl [3-{2-([4-{(tert-butyldiphenylsilyl)oxy}benzyl] oxy)-4,6-dimethylphenyl}-1-hydroxy-3-methylbutan-2-yl]carbamate (**6**).* Glacial acetic acid (6.0 mL) and H_2O (2.1 mL) were added to a solution of silyl ether **5** (298 mg, 0.381 mmol) in THF (2.1 mL). The reaction mixture was stirred for 9 h. After addition of water followed by extraction with EtOAc, the organic layer was washed with water and brine, dried over Na_2SO_4, and concentrated in vacuo. The crude product was purified by column chromatography (hexanes/EtOAc=4/1 then 2/1 (v/v)) and 258 mg of alcohol **6** (0.386 mmol, quant.) was obtained as a white amorphousness: $[\alpha]_D^{21}$ −6.10 (*c* 1.04, $CHCl_3$); ^1H NMR ($CDCl_3$, 400 MHz) δ=1.11 (9H, s), 1.36 (9H, s), 1.45 (6H, s), 2.20 (3H, s), 2.49 (3H, s), 3.45 (1H, dd, *J*=9.7 and 7.8 Hz), 3.59 (1H, d, *J*=9.7 Hz), 4.35 (1H, dd, *J*=8.5 and 7.8 Hz), 4.89 (1H, d, *J*=11.7 Hz), 4.93 (1H, d, *J*=11.7 Hz), 5.05 (1H, d, *J*=8.5 Hz), 6.56 (1H, s), 6.60 (1H, s), 6.77 (2H, d, *J*=8.3 Hz), 7.17 (2H, d, *J*=8.3 Hz), 7.34–7.46 (6H, m), 7.70–7.74 (4H, m); ^{13}C NMR ($CDCl_3$, 75 MHz) δ=19.4, 20.7, 25.9, 26.5, 28.3, 29.2, 43.5, 59.4, 64.5, 70.9, 79.2, 112.6, 119.9, 127.6, 127.7, 129.1, 129.3, 129.9, 130.3, 132.8, 135.5, 136.4, 138.3, 155.4, 157.3, 158.5; IR (KBr) 701, 823, 921, 1171, 1253, 1511, 1695, 2860, 2931, 2961 cm^{-1}; HRMS (ESI-TOF) *m/z* calcd for $C_{41}H_{54}NO_5Si$ ($[M+H]^+$) 668.3771, found 668.3797.

*4.2.3. (S)-2-([{(9H-Fluoren-9-yl)methoxy}carbonyl]amino)-3-{2-([4-{(tert-butyldiphenylsilyl)oxy}benzyl]oxy)-4,6-dimethylphenyl}-3-methylbutanoic acid (**3**).* To a solution of oxalyl chloride (38.0 μL, 0.444 mmol) in CH_2Cl_2 (3.6 mL) were added DMSO (63.1 μL, 0.888 mmol) and alcohol **6** (198 mg, 0.296 mmol) in CH_2Cl_2 (660 μL) slowly at −78 °C, and the resulting solution was stirred at −40 °C for 30 min. After addition of triethylamine (206 μL, 1.48 mmol) followed by stirring for 30 min at the same temperature, the reaction mixture was stirred at room temperature for an additional 30 min. Then the reaction was quenched by the addition of water and the obtained mixture was extracted with CH_2Cl_2. The organic layer was washed with satd NH_4Cl aq, dried over Na_2SO_4, and concentrated in vacuo. To a solution of the crude product in acetone/*tert*-BuOH/water (6/4/1 (v/v), 10 mL) were added 2-methyl-2-butene (212 μL, 2.00 mmol), NaH_2PO_4 (53.3 mg, 0.444 mmol), and $NaClO_2$ (176 mg, 1.55 mmol). The resulting mixture was stirred for 2.5 h. Following to the addition of satd NH_4Cl aq, the mixture was extracted with EtOAc. The resulting organic layer was dried over Na_2SO_4 and concentrated in vacuo. To the crude product in CH_2Cl_2 (6.3 mL) were added 2,6-lutidine (207 μL, 1.78 mmol) and TBSOTf (272 μL, 1.18 mmol), and the reaction mixture was stirred at room temperature for 2 h. The resulting mixture was concentrated in vacuo, and the obtained residue was dissolved in MeCN/10% (w/v) Na_2CO_3 aq (3/1 (v/v), 6.3 mL). To the resulting solution was added FmocOSu (120 mg, 0.355 mmol), and the reaction mixture was stirred at room temperature overnight. After the addition of 5% (w/v) $KHSO_4$ aq, the mixture was extracted with diethyl ether. The obtained organic layer was washed with brine, dried over Na_2SO_4, and concentrated in vacuo. The crude material was purified by column chromatography ($CHCl_3$) and 103 mg of Fmoc derivative **3** (0.128 mmol, 43%) was obtained as a beige amorphousness: $[\alpha]_D^{22}$ −5.58 (*c* 0.64, $CHCl_3$); ^1H NMR ($CDCl_3$, 400 MHz) δ=1.06 (9H, s), 1.57 (6H, s), 2.15 (3H, s), 2.47 (3H, s), 4.05–4.13 (1H, m), 4.15 (1H, dd, *J*=10.5 and 6.8 Hz), 4.28 (1H, dd, *J*=10.5 and 6.8 Hz), 4.93 (2H, s), 5.28 (1H, d, *J*=9.5 Hz), 5.56 (1H, d, *J*=9.5 Hz), 6.51 (1H, s), 6.57 (1H, s), 6.74 (2H, d, *J*=8.0 Hz), 7.18 (2H, d, *J*=8.0 Hz), 7.20–7.44 (10H, m), 7.48 (1H, d, *J*=7.5 Hz), 7.67 (4H, d, *J*=6.8 Hz), 7.70 (2H, d, *J*=7.5 Hz); ^{13}C NMR ($CDCl_3$, 75 MHz) δ=19.4, 20.8, 25.7, 26.5, 28.3, 28.8, 44.1, 47.1, 60.2, 66.8, 70.7, 112.5, 119.8, 119.9, 119.9, 125.1, 125.1, 127.0, 127.6, 127.7, 128.3, 129.0, 129.4, 129.8, 132.8, 135.5, 136.9, 137.9, 141.2, 143.9, 155.3, 156.0, 158.5, 175.6; IR (KBr) 706, 742, 757, 823, 918, 1255, 1511, 1717, 2858, 2934, 3028 cm^{-1}; HRMS (ESI-TOF) *m/z* calcd for $C_{51}H_{53}NO_6NaSi$ ($[M+Na]^+$) 826.3540, found 826.3577.

4.3. Preparation of the FR traceable linker (7)

The traceable linker was constructed on glycine-preloaded 2-chlorotrityl resin (0.87 mmol amine/g, 20 mg, 17 μmol). Coupling conditions for **8**,[20] **9**,[21] **10**, and biotin: 3 equiv building block, 3 equiv DIC, and 3 equiv HOBt·H_2O in DMF, 2 h, room temperature. Coupling conditions for **3**: 1.2 equiv **3**, 1.2 equiv HATU, 1.2 equiv DIEA in DMF (preactivated for 1 min), 2 h, room temperature. Removal of Fmoc group: 20% (v/v) piperidine in DMF, 2 min first treatment followed by washing and subsequent second treatment for 8 min, room temperature. Cleavage from resin (20 mg): TFE/AcOH/CH_2Cl_2 (1/1/3 (v/v)), 1 mL, 2 h, room temperature. Work-up: after removal of solvent under vacuo, MeCN/H_2O (1/1 (v/v)) was added to the resulting mixture. Following the removal of the resin by filtration, the solution was subjected to HPLC purification to yield traceable linker **7** as a white lyophilized powder (2.6 mg, 12%). Analytical HPLC conditions: linear gradient of solvent B in solvent A, 50–90% over 30 min. Retention time=24.3 min. Semi-preparative HPLC conditions: linear gradient of solvent B in solvent A, 50–90% over 30 min. LRMS (ESI-Ion Trap) *m/z* calcd for $C_{62}H_{85}N_{10}O_{13}SSi$ ($[M+H]^+$) 1237.6, found 1237.2.

4.4. Click chemistry of traceable linker with model peptide (12)

To a solution of traceable linker **7** (0.1 μmol) and peptide **11** (0.1 μmol) in H_2O/*tert*-BuOH (1/1 (v/v), 100 μL) were added $CuSO_4·H_2O$ (0.06 μmol) and sodium ascorbate (0.5 μmol), and the reaction mixture was shaken at room temperature for 1 h. Reaction progress was monitored by analytical HPLC. Analytical HPLC conditions: linear gradient of solvent B in solvent A, 5–90% over 30 min. Conjugate **12**: retention time=23.1 min. LRMS (ESI-Ion Trap) *m/z* calcd for $C_{101}H_{142}N_{24}O_{21}SSi$ ($[M+2H]^{2+}$) 1043.5, found 1043.2.

4.5. Fluoride-induced cleavage of the traceable linker followed by labeling (13–16)

Peptide-traceable linker conjugate **12** (0.1 μmol) in phosphate buffer containing 6 M guanidine hydrochloride and 0.05 mM EDTA (200 mM phosphate, pH 7.6, 100 μL) was treated with KF

(10 μmol) and MESNa (10 μmol). After incubation at 37 °C for 12 h, 3-bromobenzaldehyde (0.1 μmol) was added to the reaction mixture. Progress of the reaction was monitored by HPLC. Analytical HPLC conditions: linear gradient of solvent B in solvent A, 5–90% over 30 min. Intermediate **13**: retention time=16.5 min, LRMS (ESI-Ion Trap) *m/z* calcd for $C_{85}H_{123}N_{24}O_{21}S$ ($[M+H]^+$) 1847.9, found 1847.3. Biotin derivative **14**: retention time=20.2 min, LRMS (ESI-Ion Trap) *m/z* calcd for $C_{29}H_{43}N_4O_7S$ ($[M+H]^+$) 591.3, found 591.1. Aminooxy derivative **15**: retention time=11.2 min, LRMS (ESI-Ion Trap) *m/z* calcd for $C_{49}H_{75}N_{20}O_{13}$ ($[M+H]^+$) 1151.6, found 1151.2. Labeled derivative **16**: retention time=15.4 min, LRMS (ESI-Ion Trap) *m/z* calcd for $C_{56}H_{78}BrN_{20}O_{13}$ ($[M+H]^+$) 1317.5 (^{71}Br derivative) and 1319.3 (^{81}Br derivative), found 1317.1 and 1319.3.

4.6. Preparation of siloxybenzyl chloride 17 (Scheme 3)

Thionyl chloride (0.80 mL, 11 mmol) was slowly added to a solution of alcohol **4**[17] (2.0 g, 5.2 mmol) in CH_2Cl_2 (12 mL) at 0 °C, and the solution stirred for 2 h at room temperature. After the addition of ice, the reaction mixture was extracted with EtOAc. The organic layer was washed with saturated aqueous solution of $NaHCO_3$ followed by brine, dried over $MgSO_4$, and concentrated in vacuo. Chloride **17** was obtained as a white solid (1.4 g, 70%) and was used without further purification. Mp 77–79 °C; ^1H NMR ($CDCl_3$, 400 MHz) δ=1.09 (9H, s), 4.48 (2H, s), 6.73 (2H, d, J=8.5 Hz), 7.11 (2H, d, J=8.5 Hz), 7.34–7.45 (6H, m), 7.68–7.72 (4H, m); ^{13}C NMR ($CDCl_3$, 75 MHz) δ=19.4, 26.2, 26.4, 46.2, 119.8, 127.8, 129.7, 129.9, 132.6, 135.4, 155.6; IR (KBr) 704, 919, 1115, 1258, 1510, 1605, 2858, 2932, 2960, 3070 cm^{-1}; HRMS (ESI-TOF) *m/z* calcd for $C_{23}H_{26}OSiCl$ ($[M+H]^+$) 381.1441, found 381.1457; Anal. Calcd for $C_{23}H_{25}OSiCl$: C, 6.61; H, 72.51. Found: C, 6.63; H, 72.39.

4 17

Scheme 3. Reagents and conditions: (i) $SOCl_2$, CH_2Cl_2, 70%.

Acknowledgements

This research was supported in part by PRESTO, Japan Science and Technology Agency (JST) and a Grant-in-Aid for Scientific Research (KAKENHI) including Innovative Areas 'Fusion Material' and 'ChemBioChem' (24590010, 25107724, and 24102521). Takeda Pharmaceutical Company and Astellas Foundation for Research on Metabolic Disorders are also acknowledged. J.Y. and M.D. are grateful for Japan Society for the Promotion of Science fellowships. A propargyl glycine used in this study was a gift from Nagase & Co., Ltd.

Supplementary data

Supplementary data related to this article can be found at http://dx.doi.org/10.1016/j.tet.2014.05.110.

References and notes

1. Recent reviews: (a) Lapinsky, D. J. *Bioorg. Med. Chem.* **2012**, *20*, 6237–6247; (b) Dubinsky, L.; Krom, B. P.; Meijler, M. M. *Bioorg. Med. Chem.* **2012**, *20*, 554–570; (c) Li, N.; Overkleeft, H. S.; Florea, B. I. *Curr. Opin. Chem. Biol.* **2012**, *16*, 227–233; (d) Wang, K.; Yang, T.; Wu, Q.; Zhao, X.; Nice, E. C.; Huang, C. *Exp. Rev. Proteomics* **2012**, *9*, 293–310; (e) Cravatt, B. F.; Wright, A. T.; Kozarich, J. W. *Annu. Rev. Biochem.* **2008**, *77*, 383–414.
2. (a) Kotzyba-Hibert, F.; Kapfer, I.; Goeldner, M. *Angew. Chem., Int. Ed. Engl.* **1995**, *34*, 1296–1312; (b) Fleming, S. A. *Tetrahedron* **1995**, *51*, 12479–12520.
3. (a) Savage, M. D. *BioMethods* **1996**, *7*, 1–29; (b) Hofmann, K.; Kiso, Y. *Proc. Natl. Acad. Sci. U.S.A.* **1976**, *73*, 3516–3518.
4. Green, N. M. *Adv. Protein Chem.* **1975**, *29*, 85–133.
5. Recent reviews: (a) Bielski, R.; Witczak, Z. *Chem. Rev.* **2013**, *113*, 2205–2243; (b) Leriche, G.; Chisholm, L.; Wagner, A. *Bioorg. Med. Chem.* **2012**, *20*, 571–582.
6. (a) Verhelst, S. H. L.; Fonovic, M.; Bogyo, M. *Angew. Chem., Int. Ed.* **2007**, *46*, 1284–1286; (b) Paulick, M. G.; Hart, K. M.; Brinner, K. M.; Tjandra, M.; Charych, D. H.; Zuckermann, R. N. *J. Comb. Chem.* **2006**, *8*, 417–426; (c) van der Veken, P.; Dirksen, E. H. C.; Ruijter, E.; Elgersma, R. C.; Heck, A. J. R.; Rijkers, D. T. S.; Slijper, M.; Liskamp, R. M. J. *ChemBioChem* **2005**, *6*, 2271–2280.
7. Yamamoto, J.; Denda, M.; Maeda, N.; Kita, M.; Komiya, C.; Tanaka, T.; Nomura, W.; Tamamura, H.; Sato, Y.; Yamauchi, A.; Shigenaga, A.; Otaka, A. *Org. Biomol. Chem.* **2014**, *12*, 3821–3826.
8. Equlibrium-based hydrazone type linkers designed for purification and labeling of the target protein as similar to the traceable linker, see: (a) Dirksen, A.; Yegneswaran, S.; Dawson, P. E. *Angew. Chem., Int. Ed.* **2010**, *49*, 2023–2027; (b) Park, K. D.; Liu, R.; Kohn, H. *Chem. Biol.* **2009**, *16*, 763–772.
9. (a) Shigenaga, A.; Ogura, K.; Hirakawa, H.; Yamamoto, J.; Ebisuno, K.; Miyamoto, L.; Ishizawa, K.; Tsuchiya, K.; Otaka, A. *ChemBioChem* **2012**, *13*, 968–971; (b) Shigenaga, A.; Hirakawa, H.; Yamamoto, J.; Ogura, K.; Denda, M.; Yamaguchi, K.; Tsuji, D.; Itoh, K.; Otaka, A. *Tetrahedron* **2011**, *67*, 3984–3990; (c) Shigenaga, A.; Yamamoto, J.; Sumikawa, Y.; Furuta, T.; Otaka, A. *Tetrahedron Lett.* **2010**, *51*, 2868–2871; (d) Shigenaga, A.; Yamamoto, J.; Hirakawa, H.; Ogura, K.; Maeda, N.; Morishita, K.; Otaka, A. *Tetrahedron Lett.* **2010**, *51*, 2525–2528; (e) Shigenaga, A.; Tsuji, D.; Nishioka, N.; Tsuda, S.; Itoh, K.; Otaka, A. *ChemBioChem* **2007**, *8*, 1929–1931.
10. (a) Milstien, S.; Cohen, L. A. *Proc. Natl. Acad. Sci. U.S.A.* **1970**, *67*, 1143–1147; (b) Levine, M. N.; Raines, R. T. *Chem. Sci.* **2012**, *3*, 2412–2420 and references therein.
11. Ulrich, S.; Boturyn, D.; Marra, A.; Renaudet, O.; Dumy, P. *Chem.—Eur. J.* **2014**, *20*, 34–41.
12. (a) Anderson, E. *Chem. Biol. Interact.* **1998**, *112*, 1–14 and references therein; (b) Jones, D. P.; Carlson, J. L.; Samiec, P. S.; Sternberg, P.; Mody, V. C.; Reed, R. L.; Brown, L. A. S. *Clin. Chim. Acta* **1998**, *275*, 175–184.
13. Itai, K.; Onoda, T.; Nohara, M.; Ohsawa, M.; Tanno, K.; Sato, T.; Kuribayashi, T.; Okayama, A. *Clin. Chim. Acta* **2010**, *411*, 263–266 and references therein.
14. Wuts, P. G. M.; Greene, T. W. *Greene's Protective Group in Organic Synthesis*, 4th ed.; John Wiley & Sons: Hoboken, NJ, 2007.
15. Shigenaga, A.; Yamamoto, J.; Nishioka, N.; Otaka, A. *Tetrahedron* **2010**, *66*, 7367–7372.
16. A review of fluoride sensors including the use of the siloxybenzyl unit, see: Zhou, Y.; Zhang, J. F.; Yoon, J. *Chem. Rev.* **2014**, *114*, 5511–5571. http://dx.doi.org/10.1021/cr400352m.
17. Pettit, G. R.; Grealish, M. P.; Jung, M. K.; Hamel, E.; Pettit, R. K.; Chapuis, J.-C.; Schmit, J. M. *J. Med. Chem.* **2002**, *45*, 2534–2542.
18. Tsunoda, T.; Otsuka, J.; Yamamiya, Y.; Ito, S. *Chem. Lett.* **1994**, *23*, 539–542.
19. Sakaitani, M.; Ohfune, Y. *J. Org. Chem.* **1990**, *55*, 870–876.
20. Katayama, H.; Hojo, H.; Ohira, T.; Nakahara, Y. *Tetrahedron Lett.* **2008**, *49*, 5492–5494.
21. Cipolla, L.; Rescigno, M.; Leone, A.; Peri, F.; Ferla, B. L.; Nicotra, F. *Bioorg. Med. Chem.* **2002**, *10*, 1639–1646.
22. Recent examples of MS analyses utilizing isotope pattern of bromine: (a) Liu, H.; Lichti, C. F.; Mirfattah, B.; Frahm, J.; Nilsson, C. L. *J. Proteome Res.* **2013**, *12*, 4248–4254; (b) Hudson, S. R.; Chadbourne, F. L.; Helliwell, P. A.; Pflimlin, E.; Thomas-Oates, J. E.; Routledge, A. *ACS Comb. Sci.* **2012**, *14*, 97–100.
23. Peptide **11** was treated with KF, MESNa, and 3-bromobenzaldehyde in Na phosphate buffer (pH 7.6) containing guanidine hydrochloride and EDTA, but no reaction was observed (Fig. S3 in the Supplementary data). This result also supports that the aldehyde was incorporated onto the aminooxy group but not onto the amino group.
24. It was confirmed by co-injecting the reaction mixture of 4-(*tert*-butyldiphenylsiloxy)benzyl chloride **17** with KF and MESNa in phosphate buffer. Preparation of **17** is described in Scheme 3 of the Experimental section.

Tetrahedron 70 (2014) 4400–4404

Contents lists available at ScienceDirect

Tetrahedron

journal homepage: www.elsevier.com/locate/tet

Development of the 8-aza-3-bromo-7-hydroxycoumarin-4-ylmethyl group as a new entry of photolabile protecting groups

Hikaru Takano [a], Tetsuo Narumi [a,*,†], Nami Ohashi [a], Akinobu Suzuki [b], Toshiaki Furuta [b], Wataru Nomura [a], Hirokazu Tamamura [a,*]

[a] Institution of Biomaterial and Bioengineering, Tokyo Medical and Dental University, 2-3-10 Kandasurugadai, Chiyoda-ku, Tokyo 101-0062, Japan
[b] Department of Biomolecular Science, Toho University, 2-2-1 Miyama, Funabashi, Chiba 274-8510, Japan

ARTICLE INFO

Article history:
Received 5 March 2014
Received in revised form 22 April 2014
Accepted 22 April 2014
Available online 30 April 2014

Keywords:
Azacoumarin
Photolabile protecting groups
Caged compounds
Photolytic efficiency
Hydrophilicity

ABSTRACT

A significant substitution effect of the position of the bromo group on the photosensitivity of the 8-azacoumarin chromophore leads to the development of a highly photosensitive 8-aza-3-bromo-7-hydroxycoumarin-4-ylmethyl (aza-3-Bhc) group that shows excellent photolytic efficiency and hydrophilicity with long-wavelength absorption maxima. The newly identified aza-3-Bhc group can be applied to caged glutamates for ester-type and carbamate-type protections of carboxyl and amino functionalities.

1. Introduction

Photosensitive biologically active compounds (referred to as caged compounds) have attracted considerable attention due to their practical potentials as phototriggers of biological functions.[1] Progress in the field has been driven by the development of new photolabile protecting group types,[2] such as nitrobenzyl,[3] benzoin,[4] phenacyl,[5] and coumarin.[6] Although a number of chromophores have been applied to photolabile protecting groups, 8-azacoumarin derivatives have not been applied to the caged compounds until our identification of several advantages as an attractive chromophore for caging chemistry, such as excellent water solubility, high molar absorptivity, and efficient photorelease at low pH as described in our previous report.[7] This report describes the unexpected substitution effects on the photosensitivity of 8-azacoumarin chromophore, leading to the development of a novel 8-aza-3-bromo-7-hydroxycoumarin-4-ylmethyl caging group (aza-3-Bhc **1**) that shows excellent photolytic efficiency and hydrophilicity with long-wavelength absorption maxima and high molar absorptivity, whose features are superior to those of the 6-bromo derivatives **2** (Fig. 1).

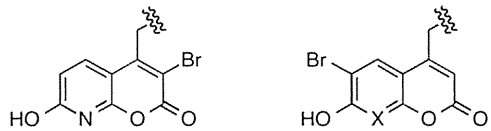

1 *aza-3-Bhc*

2a, *Bhc* (X = CH)
2b, *aza-Bhc* (X = N)

Fig. 1. Structures of azacoumarin- and coumarin-based Bhc groups.

2. Results and discussion

Our study on the development of the aza-3-Bhc group emerged from the bromination of azacoumarin derivative **3** that provided the 6-brominated compound **4a** in a 67% yield as a major product,[7] accompanied with a 16% yield of the 3-brominated compound **4b** as a minor product (Scheme 1a, Supplementary data). Bromination of the coumarin chromophore provides several advantages for photolysis reactions including lowering the pK_a of the adjacent hydroxyl group accelerating the formation of the strongly absorbing anion and the promotion of intersystem crossing to the triplet, which is considered to be the photochemically reactive state.[6d]

* Corresponding authors. Tel./fax: +81 53 478 1198 (T.N.); tel.: +81 3 5280 8036; fax: +81 3 5280 8039 (H.T.); e-mail addresses: ttnarum@ipc.shizuoka.ac.jp (T. Narumi), tamamura.mr@tmd.ac.jp (H. Tamamura).
† Present address. Department of Applied Chemistry and Biochemical Engineering, Faculty of Engineering, Shizuoka University, Hamamatsu, Shizuoka 432-8561, Japan.

0040-4020/$ – see front matter © 2014 Elsevier Ltd. All rights reserved.
http://dx.doi.org/10.1016/j.tet.2014.04.063

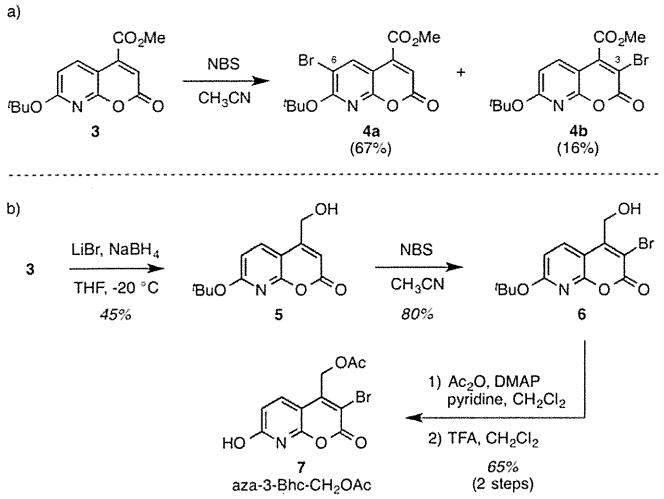

Scheme 1. Synthesis of brominated 8-azacoumarin esters **4** and aza-3-Bhc-CH_2OAc **7**.

Preliminary studies revealed that the 8-aza-7-hydroxycoumarin chromophore as well as the 6-bromo-7-hydroxycoumarin has a pK_a value, which is lower than 7.4, and mostly assumes the deprotonated (ionic) form under physiological conditions without additional electron-withdrawing groups. Therefore, the absorption spectrum of **9** has a single peak as the spectrum of **8** (Fig. 2). These features imply the possibility that the regioisomeric 3-brominated 8-azacoumarin chromophore would also work as a hydrophilic caging group. Furthermore, several papers[8] that identified strong substitution effects on quinolone chromophores prompted us to invoke that the substitution pattern could positively affect photophysical and photochemical properties of 8-azacoumarin chromophore.

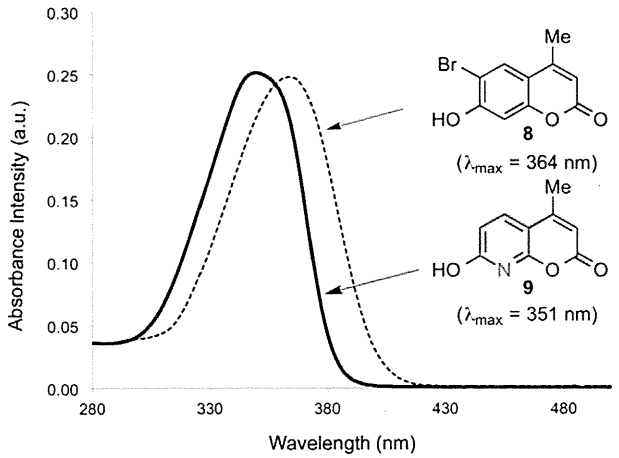

Fig. 2. Absorption spectra of Bhc derivative **8** (dash line) and 8-aza-hc **9** (solid line).

The 3-brominated acetate aza-3-Bhc-CH_2OAc **7** was synthesized from **3** in four steps (Scheme 1b). Briefly, reduction of **3** with $LiBH_4$ gave the corresponding alcohol **5** in moderate yield. In contrast with the bromination of **3** that gave a mixture of regioisomers, the bromination of alcohol **5** proceeded regioselectively to provide the 3-brominated alcohol **6** in 80% yield, which was subjected to acetylation followed by TFA treatment to give the desired aza-3-Bhc-CH_2OAc **7**.

Initially, we investigated the photophysical and hydrophilic behaviors of aza-3-Bhc-CH_2OAc **7** (Table 1). Compared with the original Bhc-CH_2OAc **11**, the absorption maximum of **7** shifted to longer wavelength from 370 nm for **11** to 378 nm for **7**, whereas that of **10** shifted to shorter wavelength (λ_{max}=362 nm). The molar absorptivity at the maximum wavelength (ε_{max}) of **7** is 27,086 M^{-1} cm^{-1}, which is also higher than those of **10** (ε_{max}=21,107 M^{-1} cm^{-1}) and **11** (ε_{max}=16,584 M^{-1} cm^{-1}). These results indicated that the 3-brominated 8-azacoumarin would be a superior chromophore to the 6-brominated coumarins. As expected, aza-3-Bhc-CH_2OAc **7** has a pK_a value below the physiological pH and also shows high aqueous solubility, which is important for the photorelease of high concentrations of the caged compounds under physiological conditions. HPLC monitoring of the hydrolysis stability revealed that while aza-3-Bhc-CH_2OAc **7** was more sensitive to hydrolysis in PBS (pH 7.4) than aza-Bhc-CH_2OAc **10**, the hydrolysis stability of **7** in KMOPS buffer (10 mM MOPS; 3-morpholinepropane-1-sulfonic acid, and 100 mM KCl, pH 7.1) is comparable to that of **10** (Fig. 3).

Table 1
Photophysical and hydrophilic properties of aza-3-Bhc-CH_2OAc **7**, aza-Bhc-CH_2OAc **10**, and Bhc-CH_2OAc **11**

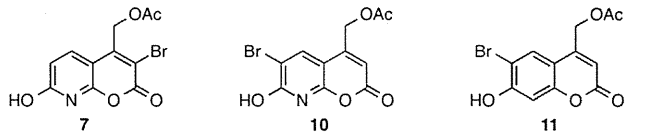

Compd	λ_{max}[a] (nm)	ε_{max}[b] (M^{-1} cm^{-1})	C_s[c] (μM)	pK_a[d]
Aza-3-Bhc-CH_2OAc (**7**)	378	27,086	3260	5.08
Aza-Bhc-CH_2OAc (**10**)	362	21,107	10,832	4.22
Bhc-CH_2OAc (**11**)	370	16,584	602	5.88

[a] Long-wavelength absorption maxima in PBS (0.1% DMSO).
[b] Molar absorptivity at the absorption maxima.
[c] Concentration at saturation in PBS (0.1% DMSO).
[d] Determined using citric/phosphate buffer in the pH range 2.6–7.0.

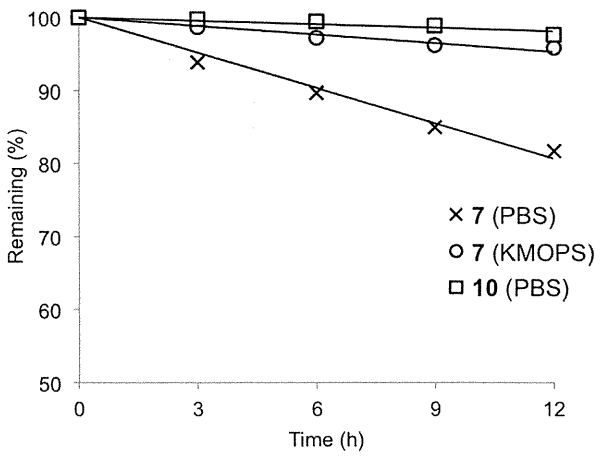

Fig. 3. Hydrolysis stability of compounds **7** and **10** at room temperature in dark. Time course of compounds **7** and **10** in PBS or KMOPS was analyzed by reversed-phase HPLC.

Having recognized promising photophysical and hydrophilic behaviors of the 3-brominated 8-azacoumarin chromophore, we evaluated the photochemical properties of aza-3-Bhc-CH_2OAc **7** under the photolysis in 5 μM KMOPS buffer solution at pH 7.2 at 350 nm. The time course of photolysis reaction of **7** was monitored by HPLC in terms of the consumption of the starting materials (Table 2), and indicates that the photolytic reaction at 350 nm of **7** follows a single-exponential decay as in the result of the original Bhc compound **11**. The time to reach 90% conversion (t_{90}) for photolysis of **7** is 19 s, which is shorter than those of the 6-

Table 2
Time course for photolysis reactions of aza-3-Bhc-CH_2OAc **7**, aza-Bhc-CH_2OAc **10**, and Bhc-CH_2OAc **11** and selected photochemical properties

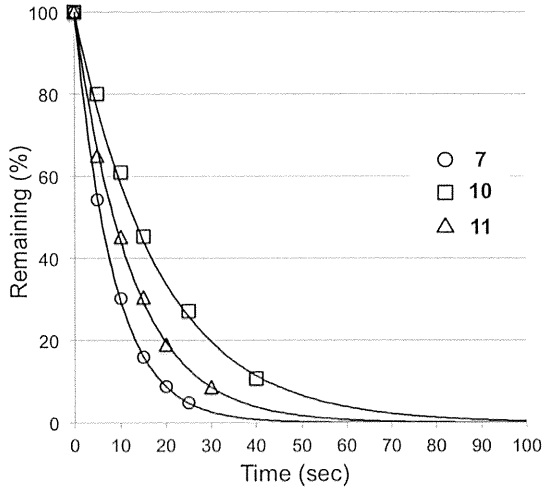

Compd	t_{90} (s)	ε_{350}[a] (M^{-1} cm^{-1})	Φ_{chem}[b]	$\varepsilon_{350}\cdot\Phi_{chem}$[c]
Aza-3-Bhc-CH_2OAc (**7**)	19	20,175	0.17	2667
Aza-Bhc-CH_2OAc (**10**)	42	20,583	0.059	1211
Bhc-CH_2OAc (**11**)	28	13,774	0.13	1806

[a] Molar absorptivity at 350 nm.
[b] Quantum yields for the disappearance of starting materials upon irradiation at 350 nm.
[c] Product of the photolysis quantum yield and molar absorptivity.

brominated coumarins **10** and **11** (t_{90}=42 s for **10** and 28 s for **11**, respectively). The photolysis quantum yields of disappearance of starting materials were calculated from the single decay curves using the equation $\Phi=1/(I\times10^3\varepsilon t_{90})$ as reported by Tsien.[9] Notably, the quantum yield of disappearance of **7** (Φ_{chem}=0.17) is approximately three times higher than that of **10** (Φ_{chem}=0.059) and significantly higher than that of **11** (Φ_{chem}=0.13). In addition, the photolytic efficiency,[10] the product of the photolysis quantum yield (Φ_{chem}) and molar absorptivity (ε) of **7** ($\varepsilon_{350}\cdot\Phi_{chem}$=2667), is approximately 1.5–2.2-fold higher than that of **10** ($\varepsilon_{350}\cdot\Phi_{chem}$=1211) and **11** ($\varepsilon_{350}\cdot\Phi_{chem}$=1806). These results indicate that the bromo substitution on position 3 of the 8-azacoumarin chromophore leads not only to improve the photophysical behavior but also to increase the photosensitivity. Although the reason for the significant enhancement of photochemical reactivity of **7** is not fully understood at this stage, these observations suggest that the aza-3-Bhc group has a powerful set of photophysical, photochemical, and hydrophilic properties for caging chemistry.

Next, we examined the synthetic methods for the introduction of the aza-3-Bhc group to biologically relevant compounds (Scheme 2). The aza-3-Bhc group is not limited to the caging group for ester-types. In addition to the α-Glu ester **12**, the aza-3-Bhc group can be applied to the α-Glu carbamate **13** for the protection of an amino functionality, which can be removed efficiently with light of wavelength of 365 nm to produce the corresponding alcohol.[11] Compared to the corresponding Bhc-protected compounds **14** and **15**,[6d] both aza-3-Bhc-protected compounds **12** and **13** showed improved photosensitivity (Table 3). The time to reach 90% conversion (t_{90}) for photolysis of **12** is 32 s, which corresponds to be approximately 20% faster than that of the corresponding Bhc-protected α-Glu ester **14** (t_{90} of **14**=38 s). A similar superiority of the aza-3-Bhc group was observed with the carbamate substrates **13** and **15**. In accordance with the greater quantum yields of disappearance and comparable molar absorptivities, the photolytic efficiency of both **12** and **13** is higher than those of **14** and **15** (relative

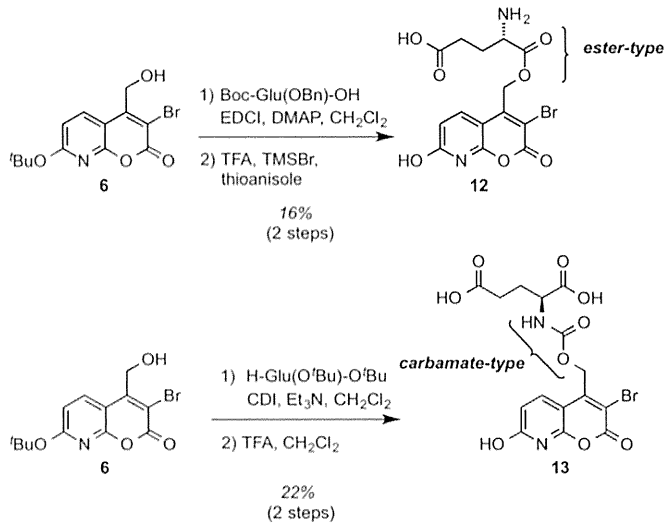

Scheme 2. Synthesis of aza-3-Bhc-caged glutamates.

value of $\varepsilon\cdot\Phi$ of **12**/**14**=1.19 and of **13**/**15**=1.27). These results indicate that the newly identified aza-3-Bhc chromophore can serve as a variant of Bhc chromophore in biologically relevant compounds. Further studies for the application of the 8-aza-3-Bhc group to the protection of other functionalities, such as alcohols, phosphoric acids, and thiols are in progress.

3. Conclusion

We have reported the development of the aza-3-Bhc group as a new entry of photolabile protecting groups for caging chemistry through the strong influence of the position of a bromo substituent on the photosensitivity of the 8-azacoumarin chromophore. The 3-brominated 8-azacoumarin **7** is considerably more efficient than the 6-brominated regioisomer **10**. Aza-3-Bhc-CH_2OAc **7** shows excellent photolytic efficiency with a bathochromic shift of the absorption maximum of 8-azacoumarin from 362 to 378 nm. Moreover, we have disclosed the potentials of the aza-3-Bhc group as protecting groups of carboxyl and amino functionalities for caged glutamates. A key to the development of the aza-3-Bhc group is the acidic azacoumarin chromophore, whose feature can provide a new opportunity to improve the photosensitivity by chemical modifications that are distinct from those in previous approaches. Efforts to elucidate the reason for the markedly enhanced photosensitivity by the 3-bromo substituent and studies on the two-photon sensitivity of the 8-azacoumarin chromophore are currently in progress.

4. Experimental section

4.1. General methods

All reactions utilizing air- or moisture-sensitive reagents were performed in dried glassware under an atmosphere of nitrogen, using commercially supplied solvents and reagents unless otherwise noted. CH_2Cl_2 was distilled from CaH_2 and stored over molecular sieves. Thin-layer chromatography (TLC) was performed on Merck $60F_{254}$ precoated silica gel plates and were visualized by fluorescence quenching under UV light and by staining with phosphomolybdic acid, *p*-anisaldehyde, or ninhydrin, respectively. Flash column chromatography was carried out using silica gel 60 N (Kanto Chemical Co., Inc.).

Table 3
Selected photophysical and photochemical properties of aza-3-Bhc-caged glutamates **12** and **13**, and Bhc-caged glutamates **14** and **15**

Compd	λ_{max}[a] (nm)	ε_{max}[b] (M^{-1} cm^{-1})	ε_{365}[c] (M^{-1} cm^{-1})	t_{90}[d] (s)	Φ_{chem}[e]	$\varepsilon_{365}\cdot\Phi_{chem}$[f]	rel. $\varepsilon\cdot\Phi$[g]
Aza-3-Bhc-Glu-ester (**12**)	378	13,648	12,153	32	0.17	2063	1.19
Aza-3-Bhc-Glu-carbamate (**13**)	376	17,068	15,623	10	0.43	6717	1.27
Bhc-Glu-ester (**14**)	370	16,912	16,466	38	0.11	1740	—
Bhc-Glu-carbamate (**15**)	370	17,822	17,636	13	0.30	5280	—

[a] Long-wavelength absorption maxima in PBS (0.1% DMSO).
[b] Molar absorptivity at the absorption maxima.
[c] Molar absorptivity at 365 nm.
[d] Time to reach 90% conversion.
[e] Quantum yields for the disappearance of starting materials upon irradiation at 365 nm.
[f] Photolytic efficiency: product of the photolysis quantum yield and molar absorptivity.
[g] Relative value of photolytic efficiency [aza-3-Bhc/Bhc]. For full experimental protocol, see Supplementary data.

4.2. Characterization data

^{1}H NMR (400 or 500 MHz) and ^{13}C NMR (125 MHz) spectra were recorded using a Bruker Avance II spectrometer with a CryoProbe. Chemical shifts are reported in δ (ppm) relative to Me_4Si (in $CDCl_3$) as internal standard. Infrared (IR) spectra were recorded on a JASCO FT/IR 4100, and are reported as wavenumber (cm^{-1}). Low- and high-resolution mass spectra were recorded on a Bruker Daltonics micrOTOF (ESI-MS) spectrometers in the positive and negative detection modes.

4.3. HPLC condition

For analytical HPLC, a Cosmosil C18-ARII column (4.6×250 mm, Nacalai Tesque, Inc., Kyoto, Japan) was employed with a linear gradient of MeCN containing 0.1% (v/v) TFA at a flow rate of 1 cm^3 min^{-1} an Agilent HP 1100 system with DAD detection (Agilent Technologies JAPAN Ltd., Tokyo, Japan) and JASCO PU-2086 plus (JASCO corporation, Ltd., Tokyo, Japan), and eluting products were detected by UV at 340 nm.

4.4. Experimental procedures of 8-azacoumarin derivatives 5, 6, 7, 12, and 13

*4.4.1. 7-(tert-Butoxy)-4-(hydroxymethyl)-2H-pyrano[2,3-b]pyridin-2-one (**5**).* A suspension of LiBr (1.09 g, 12.6 mmol) and $NaBH_4$ (410.2 mg, 10.8 mmol) in THF (36.0 mL) was stirred under nitrogen at 50 °C for 2 h, producing the solution of $LiBH_4$ (ca. 0.3 M). To the solution was added compound **3** (1.03 g, 3.72 mmol) in THF (36.0 mL), and the mixture was stirred at −20 °C for 2 h. The reaction mixture was quenched by 1 M HCl aq, and the organic layer was removed under reduced pressure. The residue was extracted with EtOAc, washed with brine, and dried over Na_2SO_4. Concentration under reduced pressure followed by flash column chromatography over silica gel with *n*-hexane/EtOAc (1:1) gave the title compound **5** (411.8 mg, 45% yield) as white powder. Mp: 236–244 °C (dec); ^{1}H NMR (500 MHz, $CDCl_3$) δ 1.64 (s, 9H), 4.85 (m, 2H), 6.45 (m, 1H), 6.60 (m, 1H), 7.74 (m, 1H); ^{13}C NMR (125 MHz, $CDCl_3$) δ 28.3, 60.9, 82.5, 104.9, 109.1, 110.5, 134.6, 153.9, 157.4, 161.5, 164.6; IR (ATR) ν 3395 (OH), 1704 (CO); HRMS (ESI), *m/z* calcd for $C_9H_8NO_4$ $[M-tert\text{-}Bu+2H]^+$ 194.0453, found 194.0450.

*4.4.2. 3-Bromo-7-(tert-butoxy)-4-(hydroxymethyl)-2H-pyrano[2,3-b]pyridin-2-one (**6**).* To a solution of compound **5** (121.4 mg, 0.487 mmol) in CH_3CN (1.37 mL) was added NBS (428.6 mg, 125 mmol), and the mixture was stirred at room temperature for 4 h. After being concentrated under reduced pressure, the residue was dissolved in EtOAc, washed with H_2O, and dried over Na_2SO_4. Concentration under reduced pressure followed by flash column chromatography over silica gel with *n*-hexane/EtOAc (1:1) gave the title compound **6** (127.1 mg, 80% yield) as a dark green solid. Mp: 254–257 °C (dec); ^{1}H NMR (500 MHz, $CDCl_3$) δ 1.64 (s, 9H), 5.02 (s, 2H), 6.67 (m, 1H), 8.13 (m, 1H); ^{13}C NMR (125 MHz, $CDCl_3$) δ 28.7, 61.9, 82.9, 106.1, 109.3, 111.3, 136.8, 150.3, 156.23, 157.7, 164.7; IR (ATR) ν 3465 (OH) 2977 (CH), 2929 (CH), 1707 (CO), HRMS (ESI), *m/z* calcd for $C_{13}H_{14}BrNNaO_4$ $[M+Na]^+$ 350.0004, found 350.0000.

*4.4.3. (3-Bromo-7-hydroxy-2-oxo-2H-pyrano[2,3-b]pyridin-4-yl) methylacetate (**7**).* To a solution of compound **6** (127.1 mg, 0.389 mmol) and DMAP (6.20 mg, 0.0507 mmol) in CH_2Cl_2 (5.6 mL) were added sequentially pyridine (313.1 μL, 3.89 mmol) and acetic anhydride (183.7 μL, 1.94 mmol), and the mixture was stirred at room temperature for 1 h. The reaction mixture was diluted with CH_2Cl_2, washed with $NaHCO_3$ aq, and dried over Na_2SO_4. Concentration under reduced pressure gave the corresponding acetate (138.1 mg, 96% yield). To a solution of the corresponding acetate (138.1 mg, 0.374 mmol) in CH_2Cl_2 (1 mL) was added trifluoroacetic acid (1 mL), and the mixture was stirred at room temperature for 30 min. Concentration under reduced pressure followed by flash column chromatography over silica gel with $CHCl_3$/MeOH (5:1) to give the title compound **7** (80.1 mg, 68% yield) as a white solid. Mp: 273–276 °C (dec); ^{1}H NMR (500 MHz, CD_3OD) δ 1.99 (s, 3H), 5.35 (s, 2H), 6.53 (d, *J*=9.0 Hz, 1H), 7.97 (d, *J*=9.0 Hz, 1H); ^{13}C NMR (125 MHz, CD_3OD) δ 20.5, 61.1, 102.0, 106.1, 109.4, 136.2, 150.9, 158.4, 160.4, 166.8, 170.0; IR (ATR) ν 2923 (OH) 1736 (CO), HRMS (ESI), *m/z* calcd for $C_{11}H_8BrNNaO_5$ $[M+Na]^+$ 335.9484, found 335.9485.

*4.4.4. (S)-4-Amino-5-((3-bromo-7-hydroxy-2-oxo-2H-pyrano[2,3-b]pyridin-4-yl)methoxy)-5-oxopentanoic acid (**12**).* To a solution of Boc-Glu(OBn)-OH (158.0 mg, 0.468 mmol), EDCI·HCl (541.2 mg, 2.82 mmol), and DMAP (13.8 mg, 0.113 mmol) in CH_2Cl_2 (10.2 mL) was added compound **6** (100.7 mg, 0.308 mmol), and the mixture was stirred at room temperature for 24 h. The mixture was poured into water and extracted with EtOAc, and dried over Na_2SO_4. Concentration under reduced pressure gave the crude compound (321.9 mg), which was used in the next step without further purification. A solution of the crude compound (321.9 mg, 0.498 mmol), 1 M TMS-Br/TFA (3.32 mL), and 1 M thioanisole/TFA (3.32 mL) was stirred at room temperature for 3 h. Purification by preparative HPLC (Gradient: 0 min, 0% CH_3CN in H_2O; 90 min, 40% CH_3CN in H_2O) followed by lyophilization to give a title compound **12** (23.7 mg, 16% yield) as a pale purple solid. Mp: 149–154 °C (dec); ^{1}H NMR (500 MHz, CD_3OD) δ 2.06 (m, 2H), 2.39 (m, 2H), 4.10 (m, 1H), 5.56 (m, 2H), 6.60 (d, *J*=8.5 Hz, 1H), 8.06 (d, *J*=8.5 Hz, 1H); ^{13}C NMR (125 MHz, CD_3OD) δ 26.6, 30.2, 53.2, 64.7, 106.3, 110.4, 112.0, 139.1, 147.5, 157.9, 158.3, 166.6, 169.9, 175.4; IR (ATR) ν 3505 (NH), 2981 (OH), 2865 (CH), 1737 (CO), 1690 (CO) 1682 (CO), HRMS (ESI), *m/z* calcd for $C_{14}H_{14}BrN_2O_7$ $[M+H]^+$ 400.9984, found 400.9981.

*4.4.5. (S)-2-((((3-Bromo-7-hydroxy-2-oxo-2H-pyrano[2,3-b]pyridin-4-yl)methoxy)carbonyl)amino)-pentanedioic acid (**13**).* To a solution

of CDI (25.4 mg, 0.157 mmol) of CH_2Cl_2 was added **6** (48.5 mg, 0.148 mmol), and the mixture stirred at 0 °C for 1 h. After H-Glu(O^tBu)-O^tBu (90.4 mg, 0.306 mmol) and Et_3N (52.3 μL, 0.375 mmol) were added, the mixture was stirred at room temperature for additional 12 h. The reaction mixture was concentrated with reduced pressure. The residue was diluted with Et_2O, and washed with water and brine, dried over Na_2SO_4. Concentration under reduced pressure gave the crude compound (168.1 mg), which was used in the next step without further purification. To a solution of the crude compound (168.1 mg, 0.275 mmol) in CH_2Cl_2 (0.90 mL) was added TFA (2.7 mL), and the mixture was stirred at room temperature for 1 h. Purification by preparative HPLC (Gradient: 0 min, 5% CH_3CN in H_2O; 90 min, 40% CH_3CN in H_2O) followed by lyophilization to give a title compound **13** (17.6 mg, 22% yield) as a pale green solid. Mp: 196–198 °C (dec); ^1H NMR (500 MHz, CD_3OD) δ 1.88 (m, 1H), 2.16 (m, 1H), 2.38 (m, 2H), 4.19 (m, 1H), 5.46 (s, 2H), 6.68 (m, 1H), 8.19 (m, 1H); ^{13}C NMR (125 MHz, CD_3OD) δ 27.8, 31.1, 54.8, 64.0, 106.3, 110.4, 110.8, 139.6, 149.4, 157.6 (2C), 158.4, 166.3, 175.2, 176.3; IR (ATR) ν 3306 (NH), 2981 (OH), 1742 (CO), 1698 (CO), HRMS (ESI), *m/z* calcd for $C_{15}H_{13}BrN_2NaO_9$ $[M+Na]^+$ 466.9702, found 466.9701.

4.5. Determination of saturated concentrations

Saturated concentrations of compounds were calculated from the standard curves that related peak area (340 nm) against known concentration of compounds in PBS.

4.6. Determination of the pK_a values

The pK_a values of compounds were estimated from the titration curves of absorbance against pH using 10 μM substrate solution in citric/phosphate buffer solution in the pH range 2.6–7.0 by adjusting the acidity with 10 μL of 2 M NaOH sequentially. The pH values were analyzed by a sensitive pH meter (HORIBA, F51).

4.7. Photolysis and quantum efficiency measurement

Into a Pyrex test tube of 12 mm diameter was placed 2 mL of 10 μM substrate solution in KMOP solution (pH 7.2) containing 0.1% DMSO. The solution was irradiated at 350 nm using four RPR 350 nm lamps (10 mJ s^{-1}). Aliquots of 10 μM were removed periodically and analyzed by HPLC. The light output for the quantum efficiencies measurement was performed using ferrioxalate actinometry.

Acknowledgements

This research was supported by the Naito Foundation, KEN10000322 (Natural Science Scholarship) and in part by a Grant-in-Aid for Young Scientist (B) from the Ministry of Education, Culture, Sports, Science, and Technology.

Supplementary data

This section presents the experimental details, and ^1H and ^{13}C NMR spectra. Supplementary data related to this article can be found at http://dx.doi.org/10.1016/j.tet.2014.04.063.

References and notes

1. (a) *Caged Compounds*; Marriot, G., Ed.Methods in Enzymology; Academic: New York, NY, 1998; Vol. 291; (b) Mayer, G.; Heckel, A. *Angew. Chem., Int. Ed.* **2006**, *45*, 4900–4921; (c) Ellis-Davies, G. C. R. *Nat. Methods* **2007**, *4*, 619–628; (d) Lee, H. M.; Larson, D. R.; Lawrence, D. S. *ACS Chem. Biol.* **2009**, *4*, 409–427.
2. (a) Brieke, C.; Rohrbach, F.; Gottschalk, A.; Mayer, G.; Heckel, A. *Angew. Chem., Int. Ed.* **2012**, *51*, 8446–8476; (b) Klán, P.; Solomek, T.; Bochet, C. G.; Blanc, A.; Givens, R.; Rubina, M.; Popik, V.; Kostikov, A.; Wirz, J. *Chem. Rev.* **2013**, *113*, 119–191.
3. Nitrobenzyl-type: (a) Engels, J.; Schlaeger, E.-J. *J. Med. Chem.* **1977**, *20*, 907–911; (b) Kaplan, J. H.; Forbush, B., III; Hoffman, J. F. *Biochemistry* **1978**, *17*, 1929–1935.
4. Benzoin-type: (a) Sheehan, J. C.; Wilson, R. M. *J. Am. Chem. Soc.* **1964**, *86*, 5277–5281; (b) Givens, R. S.; Athey, P. S.; Kueper, L. W., III; Matuszewski, B.; Xue, J. *J. Am. Chem. Soc.* **1992**, *114*, 8708–8710; (c) Hansen, K. C.; Rock, R. S.; Larsen, R. W.; Chan, S. I. *J. Am. Chem. Soc.* **2000**, *122*, 11567–11568.
5. Phenacyl-type: (a) Sheehan, J. C.; Umezawa, K. *J. Org. Chem.* **1973**, *38*, 3771–3774; (b) Givens, R. S.; Weber, J. F. W.; Jung, A. H.; Park, C.-H. *Methods Enzymol.* **1998**, *291*, 1–29; (c) Conrad, P. G., II; Givens, R. S.; Weber, J. F. W.; Kandler, K. *Org. Lett.* **2000**, *2*, 1545–1547.
6. Coumarin-type: (a) Givens, R. S.; Matuszewski, B. *J. Am. Chem. Soc.* **1984**, *106*, 6860–6861; (b) Furuta, T.; Torigai, H.; Sugimoto, M.; Iwamura, M. *J. Org. Chem.* **1995**, *60*, 3953–3956; (c) Furuta, T.; Iwamura, M. *Methods Enzymol.* **1998**, *291*, 50–63; (d) Furuta, T.; Wang, S. S. H.; Dantzker, J. L.; Dore, T. M.; Bybee, W. J.; Callaway, E. M.; Denk, W.; Tsien, R. Y. *Proc. Natl. Acad. Sci. U.S.A.* **1999**, *96*, 1193–1200; (e) Hagen, V.; Bendig, J.; Fring, S.; Eckardt, T.; Helm, S.; Reuter, D.; Kaupp, U. B. *Angew. Chem., Int. Ed.* **2001**, *40*, 1045–1048; (f) Eckardt, T.; Hagen, V.; Schade, B.; Schmidt, R.; Schweitzer, C.; Bendig, J. *J. Org. Chem.* **2002**, *67*, 703–710; (g) Geisler, D.; Kresse, W.; Wiesner, B.; Bendig, J.; Kettenmann, H.; Hagen, V. *ChemBioChem* **2003**, *4*, 162–170; (h) Nomura, W.; Narumi, T.; Ohashi, N.; Serizawa, Y.; Lewin, N. E.; Blumberg, P. M.; Furuta, T.; Tamamura, H. *ChemBioChem* **2011**, *12*, 535–539.
7. Narumi, T.; Takano, H.; Ohashi, N.; Suzuki, A.; Furuta, T.; Tamamura, H. *Org. Lett.* **2014**, *16*, 1184–1187.
8. (a) Petit, M.; Tran, C.; Roger, T.; Gallavardin, T.; Dhimane, H.; Palma-Cerda, F.; Blanchard-Desce, M.; Acher, F. C.; Ogden, D.; Dalko, P. I. *Org. Lett.* **2012**, *14*, 6366–6369; (b) Zhu, Y.; Pavlos, C. M.; Toscano, J. P.; Dore, T. M. *J. Am. Chem. Soc.* **2005**, *128*, 4267–4276; (c) Davis, M. J.; Kragor, C. H.; Reddie, K. G.; Wilson, H. C.; Zhu, Y.; Dore, T. M. *J. Org. Chem.* **2009**, *74*, 1721–1729; (d) Laras, Y.; Hugues, V.; Chandrasekaran, Y.; Blanchard-Desce, M.; Acher, F. C.; Pietrancosta, N. *J. Org. Chem.* **2012**, *77*, 8294–8302.
9. Tsien, R. Y.; Zuker, R. S. *Biophys. J.* **1986**, *50*, 843–853.
10. Brown, E. B.; Shear, J. B.; Adams, S. R.; Tsien, R. Y.; Webb, W. W. *Biophys. J.* **1999**, *76*, 489–499.
11. See Supplementary data for details.

Organic & Biomolecular Chemistry

COMMUNICATION

Development of a traceable linker containing a thiol-responsive amino acid for the enrichment and selective labelling of target proteins†

Cite this: *Org. Biomol. Chem.*, 2014, **12**, 3821

Received 24th March 2014,
Accepted 17th April 2014

DOI: 10.1039/c4ob00622d

www.rsc.org/obc

Jun Yamamoto,[a] Masaya Denda,[a] Nami Maeda,[a] Miku Kita,[a] Chiaki Komiya,[a] Tomohiro Tanaka,[b] Wataru Nomura,[b] Hirokazu Tamamura,[b] Youichi Sato,[a] Aiko Yamauchi,[a] Akira Shigenaga*[a,c] and Akira Otaka*[a]

A traceable linker that is potentially applicable to identification of a target protein of bioactive compounds was developed. It enabled not only thiol-induced cleavage of the linker for enrichment of the target protein but also selective labelling to pick out the target from contaminated non-target proteins for facile identification.

A wide variety of biologically active organic molecules, including natural products, peptides, and synthetic small molecules, exert their biological activity through specific interactions with a target biological macromolecule. Among the macromolecules present in living systems, proteins represent one of the most important target classes, with enzymes, receptors, and ion channels being of particular interest. In the fields of chemical biology and drug discovery, the identification of novel protein targets with which organic molecules such as biologically active ligands can interact is critical to understanding complex biological signalling pathways and developing novel therapeutic agents, although studies of this type can be time-consuming and laborious. The identification of a protein target involves a sequence of specific processes, including (1) effectively *'fishing'* for a target protein using a biologically active ligand as a bait; (2) enrichment of the hooked target; and (3) sequence analysis of the target by the Edman degradation or mass spectrometry.[1] For the first step, photo-affinity labelling[1a,b,2] and activity-based probe technology,[1c–e] which allow the covalent attachment of a ligand to a target of interest by photo-irradiation or chemical reaction respectively, have shown good potential in terms of their application to low affinity binding pairs. Using these approaches, the hooked target can be connected to a biotinylated linker molecule that allows it to be purified over streptavidin beads using the highly specific biotin–streptavidin interaction.[1,3] The immobilized target can then be released from the streptavidin beads for subsequent sequence analysis by attenuating the biotin–streptavidin interaction. The high affinity of this interaction ($K_d = 10^{-15}$ M),[4] however, sometimes hampers the liberation of the target from the beads, and several alternatives have been developed for the liberation of the target, including the use of a cleavable linker between the bait and biotin.[5] The use of such a linker allows for the efficient elution of the target protein from the beads *via* linker cleavage, but this approach can be limited by the contamination of the target protein with non-target proteins, which can prevent the identification of the target.[6] The development of a method that allows for the cleavage of the linker moiety to be conducted under mild conditions with generation of an orthogonal functional group that is not seen in proteins is therefore strongly desired. The use of an orthogonal functional group in this context should allow for the introduction of an isotopic or fluorescent tag that would facilitate identification of the tagged target by mass spectrometry (isotopic tag) or sodium dodecyl sulfate (SDS)-PAGE (fluorescent tag).

We recently developed a trimethyl lock[7]-based stimulus-responsive amino acid that we applied to a nuclear-cytoplasmic shuttle peptide and a hypoxia-responsive fluorophore.[8] The molecular basis of this amino acid-induced amide cleavage is shown in Fig. 1. Peptide **1**, bearing an *O*-protected stimulus-responsive amino acid, was converted to phenol **2** by exposure to an appropriate stimulus (*e.g.*, **PG** = *o*-nitrobenzyl; stimulus = UV irradiation). Subsequent lactonization of the phenol led to the cleavage of peptide **2** to give fragments **3** and **4**.

It was envisioned that the incorporation of this amide scission system into a cleavable linker would allow for the enrichment and identification of target proteins, although two additional requirements would need to be considered, including (1) the cleavage of the linker should be mediated by a reagent that does not react irreversibly with the target mole-

[a]*Institute of Health Biosciences and Graduate School of Pharmaceutical Sciences, The University of Tokushima, Shomachi, Tokushima 770-8505, Japan. E-mail: shigenaga.akira@tokushima-u.ac.jp, aotaka@tokushima-u.ac.jp*
[b]*Institute of Biomaterials and Bioengineering, Tokyo Medical and Dental University, Chiyoda-ku, Tokyo 101-0062, Japan*
[c]*JST, PRESTO, 4-1-8 Honcho, Kawaguchi, Saitama 332-0012, Japan*

† Electronic supplementary information (ESI) available: Supplementary scheme and figures, experimental section, ^{1}H NMR and MS spectra. See DOI: 10.1039/c4ob00622d

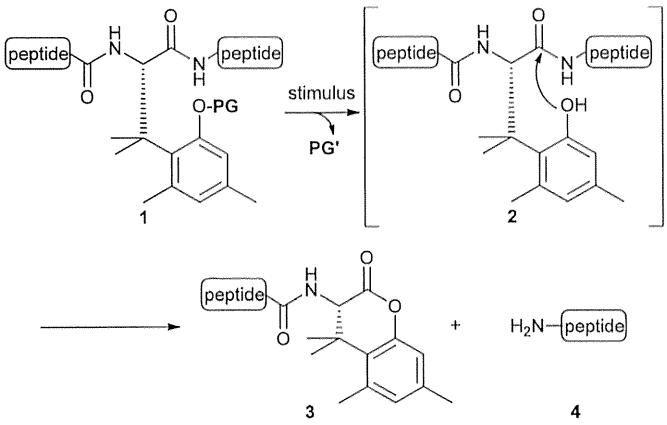

Fig. 1 Stimulus-responsive amide bond cleavage induced by a stimulus-responsive amino acid (PG: a protective group removable by an appropriate stimulus).

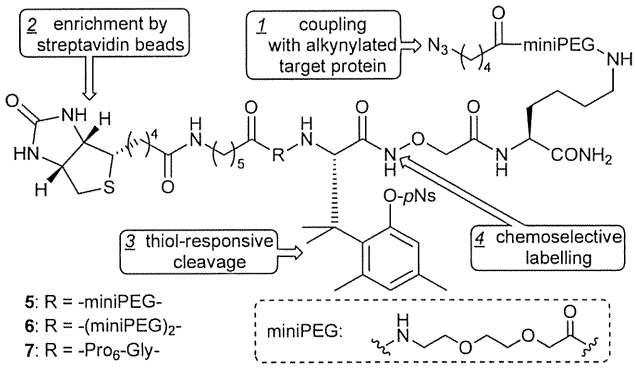

Fig. 2 Structure of traceable linkers (*p*Ns: *p*-nitrobenzenesulfonyl).

cule; and (2) it should be possible for the cleavage products to react chemoselectively during the post-cleavage labelling process to allow for the target protein to be discriminated from the contaminated non-target proteins. With these requirements in mind, we designed a new linker molecule, as shown in Fig. 2. A thiol compatible with biomolecules was used to trigger the cleavage of the linker.[9] An aminooxy moiety was used for the chemoselective labelling of the eluted target, because this functionality would react selectively with the aldehyde group on the labelling reagent.[10] An azide group was placed at one end of the linker and biotin was placed at the other to allow for the introduction of the linker into the target protein–alkyne conjugate and the enrichment of the hooked target with streptavidin beads, respectively. A general scheme depicting different functional aspects of the linker is shown in Fig. 2. The linker is initially introduced into the target protein bearing an alkynylated bait using click chemistry.[11] Following enrichment of the hooked target on streptavidin beads, the target would be eluted through a thiol-induced linker cleavage. This cleavage process would generate an aminooxy group on the target that could be chemoselectively labelled with an aldehyde derivative. Given that these linker molecules would allow for the target proteins to be traced, we named them traceable linkers. The traceable linkers would be more stable and easier to be cleaved on demand than equilibrium-based hydrazone type linkers[12] which were also designed for purification and labelling of the targets. In this study, we prepared the flexible miniPEG derivatives **5** and **6**, as well as a rigid proline-rod derivative **7**.[13]

We initially investigated the use of an enantioselective synthesis for the construction of the traceable linkers composed of a thiol-responsive amino acid. We previously reported the preparation of a racemic thiol-responsive amino acid bearing a thiol-removable *p*-nitrobenzenesulfonyl (*p*Ns) group as the

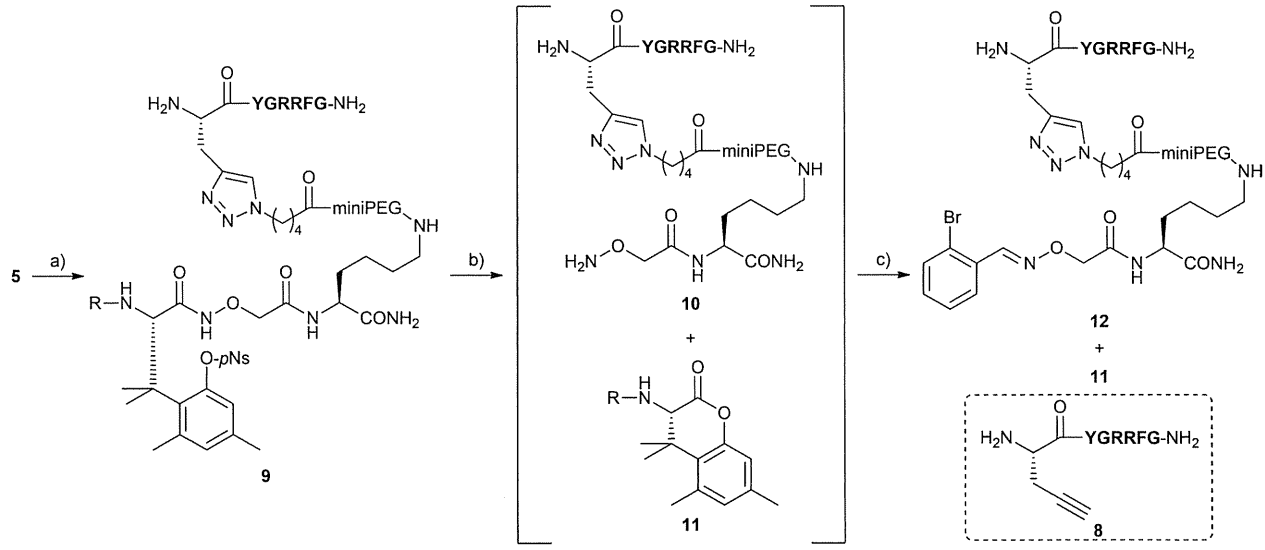

Scheme 1 Click chemistry of traceable linker **5** with model peptide **8** followed by thiol-responsive cleavage and selective labelling. Reagents and conditions: (a) **8**, $CuSO_4$, Na ascorbate, TBTA, PBS, DMSO, *tert*-BuOH; (b) 2-mercaptoethanol, NP40, Na phosphate buffer (pH 7.8), DMSO, 37 °C; (c) *o*-bromobenzaldehyde, aniline. (R: biotin–$NH(CH_2)_5CO$-miniPEG-; **F**: phenylalanine; **G**: glycine; **R**: arginine; **Y**: tyrosine).

phenolic protective group.[14] The enantioselective synthesis was therefore achieved starting from the chiral intermediate **S1** (Scheme S1 in ESI†).[15] The thiol-responsive amino acid was then incorporated into the traceable linkers using Fmoc-based solid phase peptide synthesis (Fmoc SPPS) using a 1-(4,4-dimethyl-2,6-dioxocyclohex-1-ylidene)-3-methylbutyl (ivDde) group as an ε-amino protective group.

A model reaction was conducted prior to the enrichment and selective labelling of the alkynylated protein using alkynylated peptide **8** instead of the protein (Scheme 1). Click chemistry was performed between the traceable linker **5** and the model peptide **8** in the presence of tris[(1-benzyl-1*H*-1,2,3-triazol-4-yl)methyl]amine (TBTA)[16] in phosphate buffered saline (PBS) with organic co-solvents. After 1 h of the reaction, the traceable linker–peptide conjugate **9** was generated in high purity (Fig. S1 in ESI†). We then proceeded to investigate the thiol-induced cleavage and labelling of the model peptide conjugate in a one-pot manner. The conjugate **9** was treated with 2-mercaptoethanol at 37 °C in a mixture of sodium phosphate buffer–DMSO with NP40.[17] The cleavage of the linker reached completion within 24 h to yield the model peptide **10** bearing an aminooxy group and the biotin derivative **11**. *o*-Bromobenzaldehyde was then added to the reaction mixture as a bromine-based labelling reagent[6b,18] followed by aniline, which was used to accelerate the formation of the oxime.[19] Following a reaction time of 1 h, the selective labelling of the model peptide was complete to yield the labelled peptide **12** and intact **11**.

Because the traceable linker **5** has been shown to be responsive to the thiol-induced cleavage and selective labelling processes, we proceeded to evaluate the applicability of this traceable linker strategy to the enrichment and selective labelling of an alkynylated protein. A general scheme is shown in Fig. 3A. In this study, an alkynylated enolase was used as the target protein covalently modified with the alkyne bearing substrate. The thiol-intact linker **15** was synthesized as a negative control for the thiol-induced release of the protein from the streptavidin beads (Fig. 3B). The click chemistry of linkers **5–7** and **15** was initially examined. A mixture of the alkynylated enolase and an intact one prepared according to the literature[12b] was treated with the linker in the presence of $CuSO_4$, sodium ascorbate and TBTA. SDS was also added for solubilisation of the enolase. Following a reaction time of 1 h and subsequent purification by SDS-PAGE, the biotinylated proteins and all proteins were visualized by western blot analysis using a streptavidin-horseradish peroxidase conjugate (SAv-HRP) and Lumitein staining, respectively. As shown in Fig. 4A, the linkers were successfully introduced into the enolase in all cases. It was also observed that the efficiency of the click chemistry depended on the structure of the R moiety and the amino acid on the aminooxy group. Although reason for the difference of the reactivity is not clear at present, the result suggests that optimization of not only the reaction conditions but also the structure of the linker is essential for efficient introduction of the linker onto a target protein. After the click chemistry, the proteins were treated with streptavidin beads

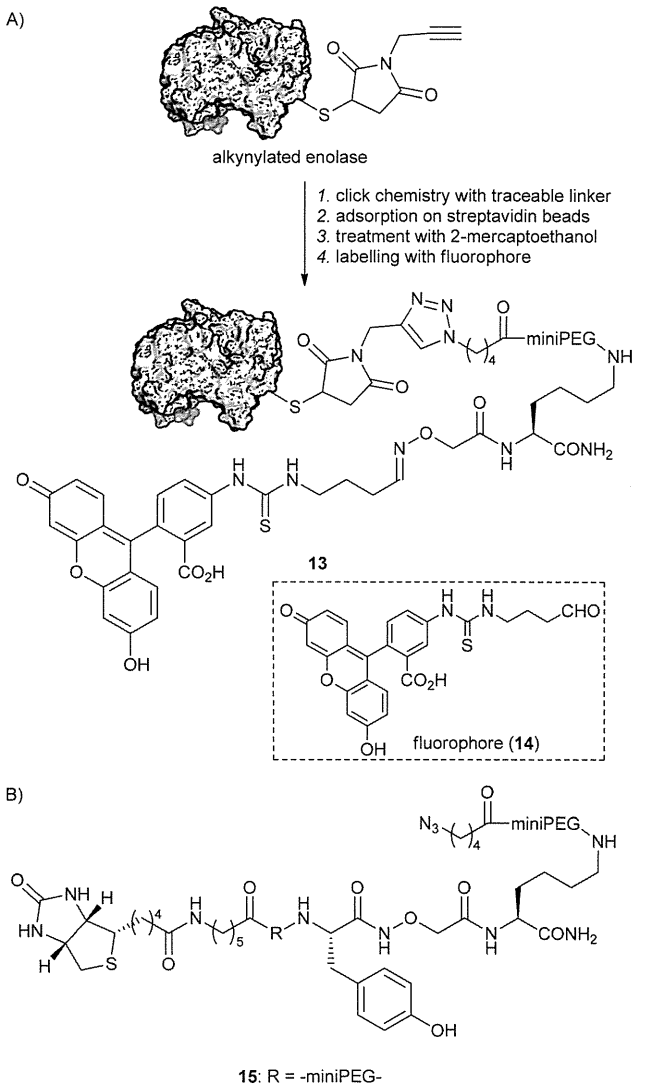

Fig. 3 (A) Schematic representation of enrichment and labelling of alkynylated enolase by traceable linker. (B) Structure of thiol-intact negative control linker **15**.

for 24 h. Following a period of washing, the beads were reacted with 2-mercaptoethanol in sodium phosphate buffer (pH 7.8) containing NP40 at 37 °C for 24 h (Fig. 3A and 4B). The resulting product was centrifuged and the supernatant was treated with the fluorophore **14**[20] in the presence of aniline for 24 h. When the traceable linker **5**, **6**, or **7** was employed, the thiol-induced elution and labelling of the enolase proceeded successfully, whereas small amounts of proteins remained on the beads after the thiol treatment (elution efficiency calculated based on Lumitein staining in Fig. 4B: 68% for **5**, 66% for **6**, and 63% for **7**).[21] In the case of the thiol-inert negative control **15**, although the enolase was successfully adsorbed onto the bead, it was not released by the thiol treatment. These observations suggested that the traceable linkers enabled the thiol-responsive release of the target protein in a similar manner to conventional cleavable linkers to allow for subsequent labelling of the aminooxy group of the

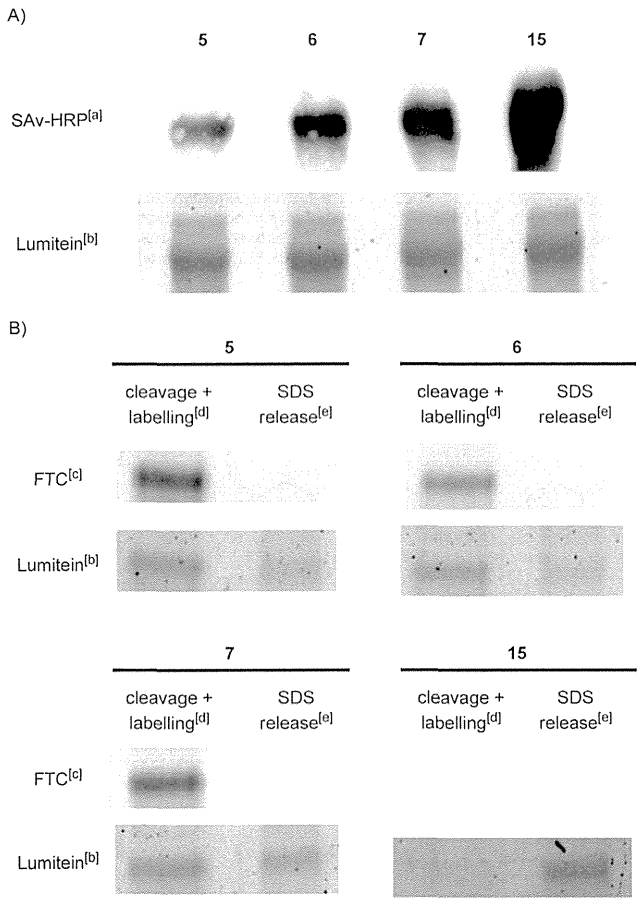

Fig. 4 Monitoring of the reactions shown in Fig. 3A using SDS-PAGE. (A) After click chemistry. Linker **5**–**7** or **15** (0.10 mM) was introduced into the alkynylated enolase (0.50 g L^{-1}) using a mixture of $CuSO_4$ (1.0 mM), Na ascorbate (0.50 mM), TBTA (0.10 mM), SDS (1% (w/v)), PBS and co-solvents over 1 h. (B) Adsorption on streptavidin beads followed by thiol-induced elution and labelling. Proteins were treated with streptavidin beads for 24 h following the click chemistry. After washing, the beads were reacted with 2-mercaptoethanol (100 mM) and NP40 (1% (v/v)) in Na phosphate buffer (10 mM, pH 7.8) at 37 °C for 24 h. The product was centrifuged and the supernatant was treated with fluorophore **14** (0.10 mM) and aniline (100 mM) for labelling. The reaction mixture was stirred for 24 h. [a] Biotinylated proteins were detected by western blotting analysis using a SAv-HRP. [b] All proteins were visualized by Lumitein staining. [c] Fluorescein-labelled proteins were detected at λ_{ex} = 488 nm and λ_{em} = 530 nm without staining. [d] Proteins after thiol treatment followed by the labelling reaction. [e] Proteins remaining on streptavidin beads after the thiol treatment. The beads after centrifugation followed by removal of the supernatant was suspended in SDS-PAGE sample loading buffer, and the resulting mixture was heated at 100 °C for 5 min. After centrifugation, the supernatant was analysed.

cleavage products. Following the enrichment and labelling processes, the traceable linker **5** gave the brightest band of all of the traceable linkers for fluorescein-labelled enolase, and this linker was therefore used in all of the subsequent experiments.

We then proceeded to investigate the orthogonal nature of the aminooxy group generated by the cleavage of the linker. The enolase–linker conjugate derived from the click chemistry with the traceable linker **5** or control **15** was treated with 2-mercaptoethanol followed by the fluorophore **14** in a similar manner to that shown in the footnote of Fig. 4. Following purification by SDS-PAGE, the labelled enolase was detected using its fluorescence tag. As shown in Fig. S3 in ESI,† labelling was only observed when the traceable linker was used. This result demonstrated that the cleaved traceable linker was suitable for the selective labelling of the target protein in the presence of other proteins.

Pull-down experiments were finally conducted for the enrichment and selective labelling of the alkynylated enolase in a protein mixture, and the results are depicted in Fig. 5. A mixture consisting of the alkynylated enolase, bovine serum albumin (BSA) and ovalbumin (1/1/1 (w/w)) was subjected to enrichment (the click chemistry with the traceable linker **5**, adsorption on streptavidin beads, and thiol treatment) and selective labelling with the fluorophore **14**. A procedure similar to that described for the alkynylated enolase shown in Fig. 4 was used in this particular case and the experimental details are provided in the ESI.† After enrichment with streptavidin beads, ovalbumin was excluded from the protein mixture as shown in Fig. 5 [Lumitein staining: proteins adsorbed on the beads before the thiol-treatment (SDS release) and proteins eluted from the beads after the thiol-treatment (cleavage + labelling)]. In this experiment, the eluent was found to be contaminated with BSA, in the same way as conventional cleavable linker systems can be contaminated with non-target proteins.[6] The eluent containing the enolase and the BSA contaminant was then treated with the fluorophore **14** in the presence of

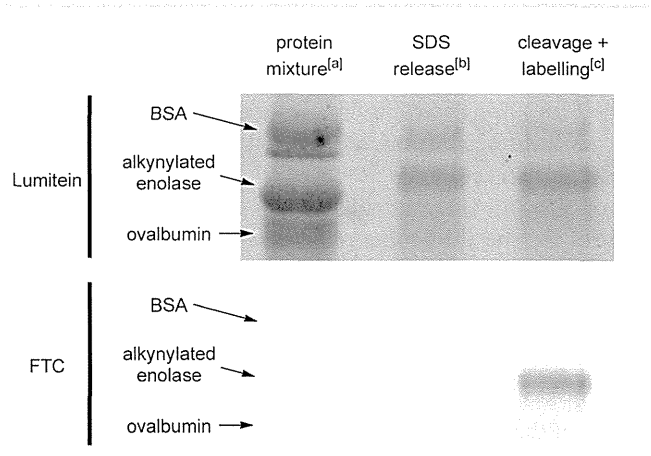

Fig. 5 Pull-down experiment for the alkynylated enolase in a protein mixture consisting of the alkynylated enolase, BSA, and ovalbumin. Enrichment (click chemistry with traceable linker **5**, adsorption on streptavidin beads, and thiol treatment) and selective labelling with fluorophore **14** were performed in a similar manner to that described in the footnote of Fig. 4. Following purification by SDS-PAGE, the labelled products or all proteins were visualized by fluorimetry without staining (FTC: λ_{ex} = 488 nm, λ_{em} = 530 nm) or Lumitein staining (Lumitein), respectively. [a] Mixture of the alkynylated enolase, BSA, and ovalbumin (1/1/1 (w/w)). [b] The beads were suspended in SDS-PAGE sample loading buffer prior to the thiol-treatment, and the mixture was heated at 100 °C for 5 min. The mixture was then centrifugated, and the supernatant was analysed. [c] Samples after enrichment and selective labelling of the alkynylated enolase.

aniline for 24 h, which resulted in the selective labelling of the enolase and allowed for the target enolase to be distinguished from the non-target contaminants (Fig. 5; FTC detection: cleavage + labelling). These results demonstrate that the traceable linker is applicable to the enrichment and selective labelling of the target protein for facile identification, even when the target protein has been contaminated with non-target proteins in the eluent obtained from the streptavidin beads.

Conclusions

In summary, we developed the traceable linker as an advanced cleavable linker. This new linker not only enabled the thiol-induced cleavage of the linker for the enrichment of the target protein in a manner similar to that of conventional cleavable linkers, but also allowed for the selective labelling of the target so that it could be distinguished from contaminated non-target proteins. Depending on an experimental design, in principle, a stimulus for cleavage of the traceable linker can be altered simply by changing a phenolic protection of the stimulus-responsive amino acid.[22] Combination of this traceable linker-based technique with the target selective introduction of an alkyne unit by the use of photo-affinity labelling or activity-based probe technology[1,2] therefore represents a new methodology for the facile clarification of the targets of the biologically active compounds, including drug candidates. The application of this traceable linker technique to the identification of the target proteins of naturally occurring bioactive compounds is currently underway in our laboratory.

Acknowledgements

This research was supported in part by PRESTO, Japan Science and Technology Agency (JST) and a Grant-in-Aid for Scientific Research from the Japanese Society for the Promotion of Science (JSPS) and the Ministry of Education, Culture, Sports, Science and Technology, Japan (MEXT). Astellas Foundation for Research on Metabolic Disorders and Takeda Pharmaceutical Company are also acknowledged. JY and MD are grateful for JSPS fellowship. A propargyl glycine used in this study was a gift from Nagase & Co., Ltd.

Notes and references

1 Recent reviews: (*a*) D. J. Lapinsky, *Bioorg. Med. Chem.*, 2012, **20**, 6237–6247; (*b*) L. Dubinsky, B. P. Krom and M. M. Meijler, *Bioorg. Med. Chem.*, 2012, **20**, 554–570; (*c*) N. Li, H. S. Overkleeft and B. I. Florea, *Curr. Opin. Chem. Biol.*, 2012, **16**, 227–233; (*d*) K. Wang, T. Yang, Q. Wu, X. Zhao, E. C. Nice and C. Huang, *Expert Rev. Proteomics*, 2012, **9**, 293–310; (*e*) B. F. Cravatt, A. T. Wright and J. W. Kozarich, *Annu. Rev. Biochem.*, 2008, **77**, 383–414.

2 (*a*) F. Kotzyba-Hibert, I. Kapfer and M. Goeldner, *Angew. Chem., Int. Ed. Engl*, 1995, **34**, 1296–1312; (*b*) S. A. Fleming, *Tetrahedron*, 1995, **51**, 12479–12520.

3 (*a*) M. D. Savage, *BioMethods*, 1996, **7**, 1–29; (*b*) K. Hofmann and Y. Kiso, *Proc. Natl. Acad. Sci. U. S. A.*, 1976, **73**, 3516–3518.

4 N. M. Green, *Adv. Protein Chem.*, 1975, **29**, 85–133.

5 Recent reviews: (*a*) R. Bielski and Z. Witczak, *Chem. Rev.*, 2013, **113**, 2205–2243; (*b*) G. Leriche, L. Chisholm and A. Wagner, *Bioorg. Med. Chem.*, 2012, **20**, 571–582.

6 (*a*) S. H. L. Verhelst, M. Fonovic and M. Bogyo, *Angew. Chem., Int. Ed.*, 2007, **46**, 1284–1286; (*b*) M. G. Paulick, K. M. Hart, K. M. Brinner, M. Tjandra, D. H. Charych and R. N. Zuckermann, *J. Comb. Chem.*, 2006, **8**, 417–426; (*c*) P. van der Veken, E. H. C. Dirksen, E. Ruijter, R. C. Elgersma, A. J. R. Heck, D. T. S. Rijkers, M. Slijper and R. M. J. Liskamp, *ChemBioChem*, 2005, **6**, 2271–2280.

7 (*a*) S. Milstien and L. A. Cohen, *Proc. Natl. Acad. Sci. U. S. A.*, 1970, **67**, 1143–1147; (*b*) M. N. Levine and R. T. Raines, *Chem. Sci.*, 2012, **3**, 2412–2420, and references therein.

8 (*a*) A. Shigenaga, D. Tsuji, N. Nishioka, S. Tsuda, K. Itoh and A. Otaka, *ChemBioChem*, 2007, **8**, 1929–1931; (*b*) A. Shigenaga, K. Ogura, H. Hirakawa, J. Yamamoto, K. Ebisuno, L. Miyamoto, K. Ishizawa, K. Tsuchiya and A. Otaka, *ChemBioChem*, 2012, **13**, 968–974.

9 Photo-cleavage reaction is also compatible with biomolecules. In this study, however, it was not used because the photo-cleavage usually generates carbonyl functionalities (*e.g.* an aldehyde from an *o*-nitrobenzyl group) that would hamper the following chemoselective labelling by reacting with an aminooxy group.

10 S. Ulrich, D. Boturyn, A. Marra, O. Renaudet and P. Dumy, *Chem. – Eur. J.*, 2014, **20**, 34–41.

11 J. E. Hein and V. V. Fokin, *Chem. Soc. Rev.*, 2010, **39**, 1302–1315, and references therein.

12 (*a*) A. Dirksen, S. Yegneswaran and P. E. Dawson, *Angew. Chem., Int. Ed.*, 2010, **49**, 2023–2027; (*b*) K. D. Park, R. Liu and H. Kohn, *Chem. Biol.*, 2009, **16**, 763–772.

13 S. Sato, Y. Kwon, S. Kamisuki, N. Srivastava, Q. Mao, Y. Kawazoe and M. Uesugi, *J. Am. Chem. Soc.*, 2007, **129**, 873–880.

14 A. Shigenaga, J. Yamamoto, H. Hirakawa, K. Ogura, K. Morishita, N. Maeda and A. Otaka, *Tetrahedron Lett.*, 2010, **51**, 2525–2528.

15 A. Shigenaga, J. Yamamoto, N. Nishioka and A. Otaka, *Tetrahedron*, 2010, **66**, 7367–7372.

16 (*a*) M. von Delius, E. M. Geertsema and D. A. Leigh, *Nat. Chem.*, 2010, **2**, 96–101; (*b*) K. Asano and S. Matsubara, *Org. Lett.*, 2010, **12**, 4988–4991; (*c*) T. R. Chan, R. Hilgraf, K. B. Sharpless and V. V. Fokin, *Org. Lett.*, 2004, **6**, 2853–2855.

17 Application of the traceable linker to a protein mixture requires that the linker cleavage and selective labelling should be performed in the presence of detergents. In this model reaction, therefore, NP-40 that is widely used as a

non-ionic detergent for solubilization of proteins was employed.

18 Recent examples of MS analyses utilizing the isotope pattern of bromine: (*a*) H. Liu, C. F. Lichti, B. Mirfattah, J. Frahm and C. L. Nilsson, *J. Proteome Res.*, 2013, **12**, 4248–4254; (*b*) S. R. Hudson, F. L. Chadbourne, P. A. Helliwell, E. Pflimlin, J. E. Thomas-Oates and A. Routledge, *ACS Comb. Sci.*, 2012, **14**, 97–100.

19 A. Sirksen, T. M. Hackeng and P. E. Dawson, *Angew. Chem., Int. Ed.*, 2006, **45**, 7581–7584.

20 E. Trevisiol, E. Defrancq, J. Lhomme, A. Laayoun and P. Cros, *Eur. J. Org. Chem.*, 2000, 211–217.

21 When the concentration of 2-mercaptoethanol was reduced to 10 mM, the linker cleavage was not observed (Fig. S2 in the ESI†). The concentration of intracellular glutathione that is the most abundant thiol in cells is 0.2 to 10 mM, therefore, our traceable linker is supposed to be compatible with proteomes with endogenous glutathione. Moreover, the glutathione and other small thiols can be removed by dialysis or ultrafiltration before the reaction with the traceable linker. For the concentration of endogenous glutathione, see: (*a*) E. Anderson, *Chem.-Biol. Interact.*, 1998, **122**, 1–14, and references therein; (*b*) D. P. Jones, J. L. Carlson, P. S. Samiec, P. Sternberg, V. C. Mody, R. L. Reed and L. A. S. Brown, *Clin. Chim. Acta*, 1998, **275**, 175–184.

22 A fluoride-responsive traceable linker has already been developed and it will be published in due course.

ASIAN JOURNAL OF ORGANIC CHEMISTRY

ACES

FULL PAPER

DOI: 10.1002/ajoc.201400026

Imidazolium Salt-Catalyzed Friedel–Crafts-Type Conjugate Addition of Indoles: Analysis of Indole/Imidazolium Complex by High Level ab Initio Calculations

Tetsuo Narumi,[a] Seiji Tsuzuki,[b] and Hirokazu Tamamura*[a]

Abstract: We describe the facile synthesis of 3-substituted indoles by Friedel–Crafts-type conjugate addition catalyzed by imidazolium salts. The reactions proceed under mild conditions with no base, solvent, or N-heterocyclic carbene. Mechanistic studies suggest the potential mechanism operates through the dual activation of indoles involving cation–π interactions of imidazolium cations with indoles and Lewis base activation by chloride anions derived from the imidazolium salts. High-level ab initio molecular orbital calculations reveal that there is a strong attraction between the imidazolium cation and the indole, and that the electrostatic and induction interactions strongly contributes to the attraction in the indole/imidazolium complex, which is a characteristic feature of the cation–π interaction.

Keywords: ab intio calculations · cation–π interactions · Friedel–Crafts reaction · imidazolium salts · indoles

Introduction

The cation–π interaction is a fundamental noncovalent interaction between cationic species and electron-rich π-electron systems.[1] The interactions of cationic species, such as inorganic ions, protonated amines, or quaternary ammonium salts, with a side chain of phenylalanine, tyrosine, or tryptophan contribute strongly to biomolecular functions, such as structural stabilization of proteins and molecular recognition.[2] Artificial systems for cation–π interactions including cyclophane molecules have been extensively studied in supramolecular and host-guest chemistry to establish the importance of the cation–π interaction.[1a,3] Amongst such systems, small molecular artificial cation–π complexes find great utility in synthetic organic chemistry, as those systems can provide potentially intriguing strategies towards reaction design.[4–7] A representative example was reported by Yamada and Morita in 2002,[4] in which an intramolecular cation–π interaction between a pyridinium cation and a benzyl moiety allows a face-selective nucleophilic addition to pyridinium salts to provide chiral 1,4-dihydropyridines. Later, Ishihara and Fushimi identified the first Cu^{2+}-based artificial metalloenzyme that is effective for the enantioselective Diels–Alder and Mukaiyama–Michael reactions,[5] in which the intramolecular cation–π interaction between the Cu^{2+} ion and the electron-rich aryl group is responsible for the transition-state assembly. In 2010, Jacobsen and co-workers reported an elegant organocatalytic system for enantioselective cationic polycyclization catalyzed by thiourea derivatives with a polycyclic aromatic group,[6] which plays a critical role for the stabilization of cation–π interactions in the transition state to achieve high levels of enantioselectivity. Furthermore, the importance of potential cation–π interactions in various organocatalytic reactions has been proposed.[7]

In this report, we document a remodeling of intermolecular cation–π interactions of imidazolium cations with indoles, which can trigger Friedel–Crafts-type conjugate additions[8] of indoles that proceed under mild conditions to provide various 3-substituted indoles (Scheme 1). Preliminary data suggest that the potential mechanism operates through the dual activation of indoles by a cation–π interaction with imidazolium cations and Lewis base activation by chloride anions derived from the imidazolium salts. High-level ab initio molecular orbital calculations support the presence of a cation–π interaction in the indole/imidazolium complex.

[a] Dr. T. Narumi,[+] Prof. Dr. H. Tamamura
Institute of Biomaterials and Bioengineering
Tokyo Medical and Dental University
Chiyoda-ku, Tokyo 101-0062 (Japan)
Fax: (+81) 3-5280-8039
E-mail: tamamura.mr@tmd.ac.jp

[b] Dr. S. Tsuzuki
Research Initiative of Computational Sciences (RICS)
Nanosystem Research Institute
National Institute of Advanced Industrial Science and Technology (AIST)
Tsukuba, Ibaraki 305-8565 (Japan)

[+] Current address:
Department of Applied Chemistry and Biochemical Engineering
Faculty of Engineering, Shizuoka University
3-5-1 Johoku, Hamamatsu 432-8561 (Japan)

Supporting information for this article is available on the WWW under http://dx.doi.org/10.1002/ajoc.201400026.

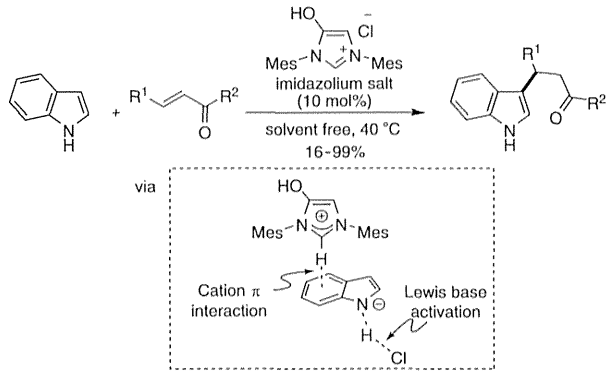

Scheme 1. Imidazolium-salt-catalyzed Friedel–Crafts-type conjugate addition through the dual activation of indole. Mes = mesityl.

Results and Discussion

Our interest in the application of imidazolium salts emerged from N-heterocyclic carbene (NHC) catalysts. Recently, considerable efforts have been made in the development of NHC catalysis, as exemplified by benzoin and Stetter reactions, homoenolate additions, and various annulation reactions of acyl azolium intermediates.[9] In contrast to these reactions, imidazolium salt-derived NHCs can also work as catalysts in Brønsted base activation. Movassaghi and Schmidt[10] reported NHC-catalyzed amidation of unactivated esters with amino alcohols via the hydrogen-bonding interaction of NHCs with alcohols, which is supported by the X-ray structure of the carbene/alcohol complex. Subsequently, Scheidt and co-workers[11] reported that the NHC (IMes) derived from IMesCl (**1a**) can effectively catalyze intermolecular conjugate additions of alcohols to activated alkenes, and Kang and Zhao[12] reported related reactions with anilines. Consideration of such reports prompted us to invoke the NHC/indole complex as a possible generated intermediate, capable of facilitating the conjugate addition of indole **2** to the conjugated acceptors.

Chalcone **3** was used as a conjugate acceptor, and while use of **1a** as a precatalyst followed by deprotonation by *n*BuLi/LiCl provided no product (Table 1, entry 1), the use of organic bases such as Et_3N, diisopropylethylamine (DIPEA), pyridine, and 1,8-diazabicyclo[5.4.0]undec-7-ene (DBU) generated the desired product **4a** in low conversion (Table 1, entries 2–5). Upon further investigation of precatalysts, solvents and bases,[13] we discovered the unique potential of imidazolium salts. In the absence of base, the reaction catalyzed by only IMesCl gave **4a** in moderate yield (Table 1, entry 6). It is also notable that the reaction under neat conditions proceeded smoothly in a higher yield (Table 1, entry 7).[14]

As examples of NHC catalysis requiring no base are scarce,[15] we examined Friedel–Crafts-type conjugate additions catalyzed by azolium salts (Table 2). The choice of azolium salts was critical. Various imidazolium salts **1a–f** are effective catalysts, and the reactions provide the desired product **4a** in low to good yields (Table 2, entries 1–7),

Table 1. Optimization of the reaction conditions.

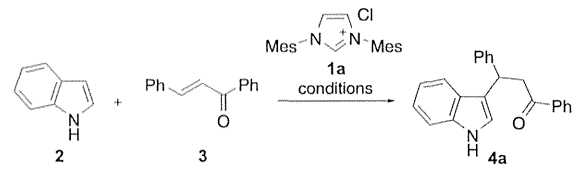

Entry	Conditions (mol %)[a]	Conv. [%][b]
1	**1a** (5), *n*BuLi (5), LiCl, toluene	nr
2	**1a**, Et_3N, CH_2Cl_2	trace
3	**1a**, DIPEA, CH_2Cl_2	7
4	**1a**, pyridine, CH_2Cl_2	8
5	**1a**, DBU, CH_2Cl_2	24
6	**1a**, no base, CH_2Cl_2	44
7	**1a**, no base, solvent-free	70

[a] Unless otherwise noted, all reactions were carried out with chalcone **3** (0.20 mmol), indole **2** (0.60 mmol, 3.0 equiv.) and IMesCl **1a** (0.02 mmol, 10 mol %) in CH_2Cl_2 (1.0 mL) at 40 °C. [b] Determined by ^1H NMR. nr = no reaction. Mes = 2,4,6-trimethylphenyl.

Table 2. Azolium salt screening for Friedel–Crafts-type conjugate additions of indoles.

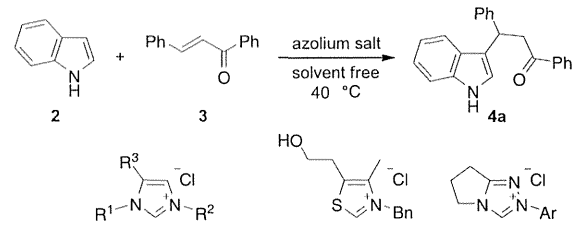

1a, $R^1 = R^2$ = Mes, R^3 = H
1b, R^1 = *n*-Bu, R^2 = Me, R^3 = H
1c, $R^1 = R^2$ = 2,6-dimethylphenyl, R = H
1d, $R^1 = R^2$ = 2,6-diethylphenyl, R = H
1e, $R^1 = R^2$ = 2,6-diisopropylphenyl, R = H
1f, $R^1 = R^2$ = Mes, R^3 = OH

6a, Ar = Mes
6b, Ar = C_6F_5

Entry	Salts	Yield [%][b]
1	**1a**	25
2	**1b**	9
3	**1c**	30
4	**1d**	36
5	**1e**	11
6	**1f**	72
7[c]	**1f**	97
8	**5**	nr
9	**6a**	nr
10	**6b**	nr
11	NH_4Cl	2
12	$BnMe_3NCl$	nr
13	Me_4NCl	nr
14	nBu_4NCl	nr

[a] Unless otherwise noted, all reactions were carried out with chalcone **3** (0.20 mmol), indole (**2**, 0.40 mmol, 2.0 equiv.) and azolium salt (0.02 mmol, 10 mol %) in solvent-free conditions at 40 °C for 12 h. [b] Yield of isolated product. [c] 24 h. nr = no reaction.

whereas a thiazolium salt **5** or triazolium salts **6** proved to be unproductive (Table 2, entries 8–10). The reaction catalyzed by ionic liquid [bmim]Cl (**1b**), which is known to be effective in the aza-Michael reaction of amines via hydrogen-bonding interactions,[14a] produced **4a** in lower yield than other imidazolium salts with N-aryl substituents, which

suggests the importance of N-aryl substituents of imidazolium salts on the reaction, and the possibility of a different reaction pathway. Furthermore, NH_4Cl and tetraalkylammonium salts were not effective (Table 2, entries 11–14), which indicates that the core structure of imidazolium salts is critical for the reaction. The best result was obtained with 4-hydroxyimidazolium salt **1f**[16] (HyMesCl), which was reported by Lavigne and co-workers, which gave the desired compound **4a** in 72% isolated yield (Table 2, entry 6). Finally, we found the optimized conditions: treatment of **3** (1.0 equiv.) with **2** (2.0 equiv.), and HyMesCl **1f** (10 mol%) at 40°C for 24 h provided **4a** in quantitative yield (Table 2, entry 7).

With the optimized condition in hand, we investigated a variety of conjugate acceptors interacting with indole (Scheme 2). The reactions with reactive substrates such as 1-phenylbutenone or β-nitrostyrene afforded the corresponding compounds **4b** and **4c**, respectively, in excellent yields, but the reaction with a highly reactive ketoester was sluggish and provided the desired compound **4d** in low yield. The sluggish reactivity of the ketoester was overcome by the use of RMesCl (**6a**), and the reaction provided **4d** in 80% yield. Replacement of the phenyl ring on the ketone with an electron-donating methyl group led to a decrease in the reactivity, but the corresponding compound **4e** was produced in moderate yield. The reaction with an enoate provided no product, but cyclic enones were effective and the desired compounds **4f** and **4g** were obtained in low to moderate yields.

Examination of the substrate scope with respect to Michael donors revealed that a methyl substituent was amenable at most positions of the indole except the C3 position, and the reactions afforded the corresponding compounds **4h–l** in moderate to high yields. Although the reaction with 3-methylindole (**7**) was resistant to catalysis by a phosphoric acid catalyst,[17,18] the reaction catalyzed by imidazolium salt **1f** afforded the desired compound **4r** in 2% yield, but also the cyclized compound **10** in 10% yield. Compound **10** is presumably produced by intramolecular cyclization of **4r** followed by olefin isomerization (Scheme 3).

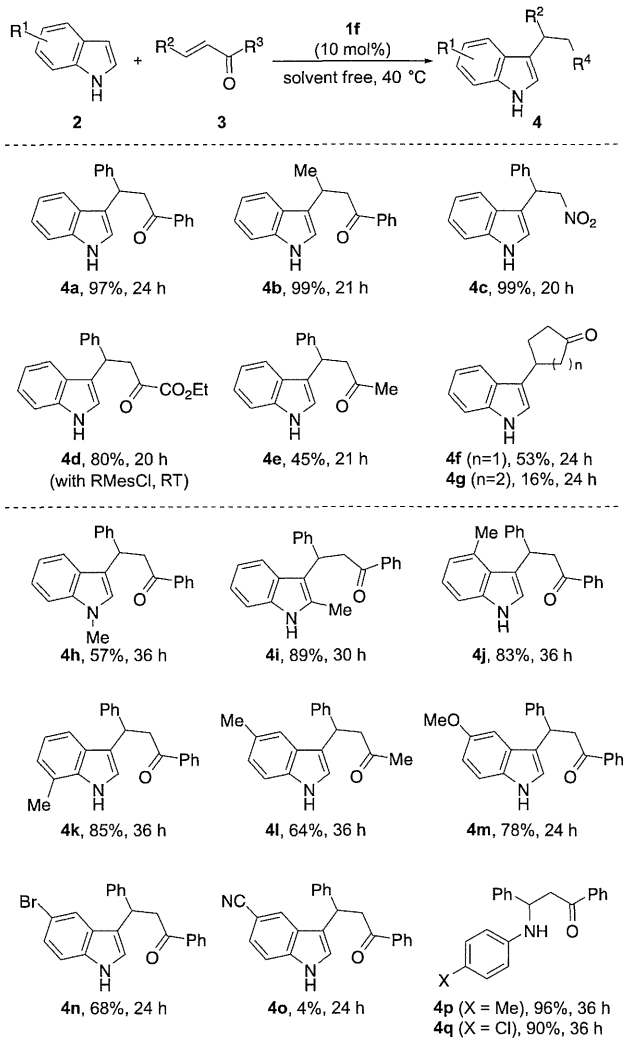

Scheme 2. Substrate scope of imidazolium salt catalyzed Friedel–Crafts-type conjugate addition.

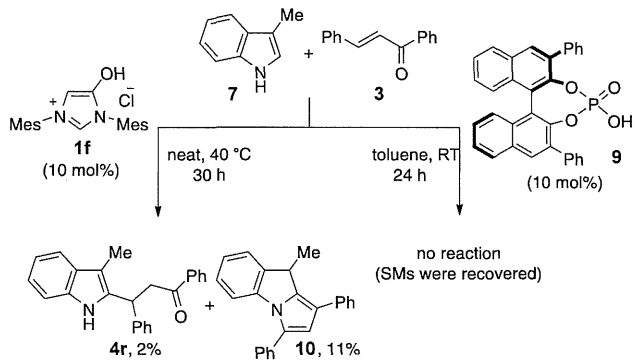

Scheme 3. Reaction with 3-methylindole.

These results demonstrate the unique nature of imidazolium salt catalysis. The reaction also tolerated an electron-donating 5-methoxy group and an electron-withdrawing 5-bromo group to produce the corresponding compounds **4m** and **4n** in 78% and 68% yield, respectively. On the other hand, the reaction of the indole substituted with a strongly electron-withdrawing 5-cyano group gave the desired indole **4o** in only 4% isolated yield. While the optimized conditions are not suited for the reactions with benzofuran and benzothiophene, aza-Michael reaction of anilines can catalyzed by **1f** to produce the corresponding compounds **4p** and **4q** in excellent yield. These results indicate the importance of a nitrogen atom in these reactions.

To gain some insight into the role played by the imidazolium salts, several mechanistic studies were performed. Counteranion studies revealed that imidazolium salts **1a**, **11a**, and **11b** with Cl^-, Br^-, and CF_3COO^- as counteranions mediate the reaction to afford **4a** in moderate conversion yields (Table 3, entries 1–3), while the use of imidazolium salts **11c** and **11d** with ClO_4^- or SbF_6^- as counter anions did not mediate the reaction (Table 3, entries 4 and

Table 3. Counteranion effects on the reaction.

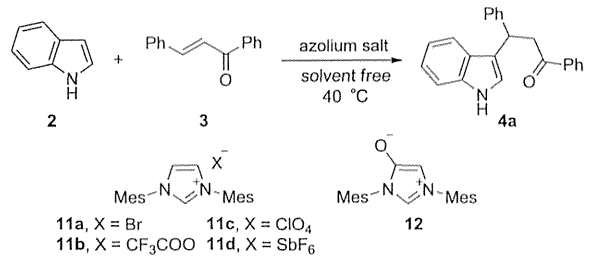

Entry	Azolium salt	Counter anion	Conv. [%][b]
1	**1a**	Cl^-	62
2	**11a**	Br^-	26
3	**11b**	CF_3COO^-	35
4	**11c**	ClO_4^-	nr
5	**11d**	SbF_6^-	nr
6	**12**	–	nr

[a] All reactions were carried out with chalcone **3** (0.20 mmol), indole (**2**, 0.40 mmol, 2.0 equiv.), and azolium salt (0.02 mmol, 10 mol%) in solvent-free conditions at 40 °C for 20 h. [b] Determined by ^{1}H NMR spectroscopy. nr = no reaction.

5). Furthermore, the reaction with zwitterionic imidazolium salt **12**[16b] that lacks a counteranion failed to provide the product (Table 3, entry 6). These results indicate that the counter anion of imidazolium salts is critical for the reaction.

However, as the pK_a value of indole is 21.0,[19] it would be difficult to deprotonate the N–H group of indoles with a chloride anion. At this stage, we speculated that some interactions induced by imidazolium salts could play an important role in the activation of indoles, leading to the formation of potential indole/imidazolium complexes that would enable the Friedel–Crafts-type conjugate addition. To investigate the interaction of indoles and imidazolium salts, the reaction was monitored by ^{1}H NMR spectroscopy. Figure 1a shows the ^{1}H NMR spectra of IMesCl (**1a**) in $CDCl_3$ (0.2 M, 20 °C) from δ = 0.00–11.0 ppm. As imidazolium groups are positively charged and have a relatively acidic C2 proton, imidazolium salts have been used as anion-binding receptors through the strong hydrogen bonding between the C2 proton of the imidazolium salt and various anions.[20] Hence, the C2 proton of **1a** is shifted significantly downfield. After treatment of **1a** with 20 equivalents of indole **2**, the C2 proton of **1a** shifted significantly upfield ($\Delta\delta$ = 1.18 ppm, Figure 1b) while no significant shift of the other protons of imidazolium ring was detected. Moreover, small upfield shifts were detected for the protons on the mesityl groups (ca. 0.23 ppm). These results indicate that treatment of **1a** with excess indole leads to a decrease in the hydrogen-bonding interactions of the imidazolium moiety with chloride anions, and also suggests that mesityl moieties of **1a** are possibly shielded by aromatic rings.

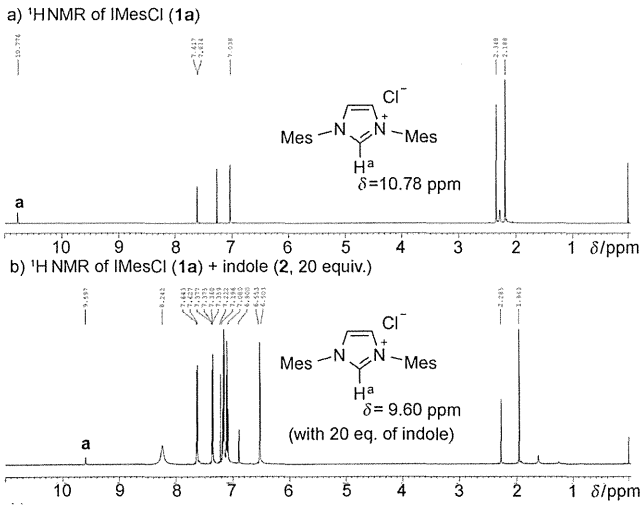

Figure 1. ^{1}H NMR investigation of the interaction of IMesCl (**1a**) and indole (**2**) in $CDCl_3$.

Furthermore, deuterium labeling studies revealed that mixing a catalytic amount of **1a** and ^{1}D-indole **2-^{1}D** (91%-*d*) in $CDCl_3$ led to immediate isomerization with deuterium incorporation at the C3 position of the indole (Scheme 4), and the reaction with ^{3}D-indole **2-^{3}D** (95%-*d*) also promoted deuterium isomerization in a similar ratio. Also, mixing an equimolar amount of IMesCl and indole in $CDCl_3$ (0.2 M, 20 °C) leads rapidly to a suspension, and forms a white precipitate within 10 min (Figure 1 in the Supporting Information). These results strongly suggest that interactions of indoles with imidazolium salts are possible in the reaction media.

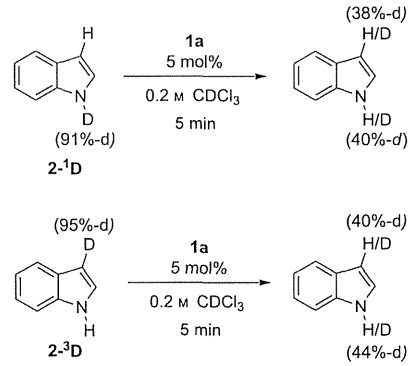

Scheme 4. IMesCl-catalyzed deuterium isomerization of *d*-indoles **2-^{1}D** and **2-^{3}D**.

Details of the interactions in indole/imidazolium complex were evaluated by ab initio calculations with Gaussian 09,[21] a powerful method for studying intermolecular interactions. Details of the computational procedures are shown in the Supporting Information.[22] If a sufficiently large basis set is used and electron correlation is properly corrected, the calculated interaction energies agree well with the gas-phase experimental values.[23] The cation–π interactions in the benzene complexes with alkali-metal and pyridinium cations have been studied[1,24] and the MP2/cc-pVTZ level interaction energy potentials calculated for 16 orientations of the indole/1,3-dimethylimidazolium complex **A**–**P** (Figure 2) are shown in Figure 3. There is a clear tendency

